ORIGINAL ARTICLE

Prospective Randomized Trial of Limbal Relaxing Incisions Combined With Microincision Cataract Surgery

Masayuki Ouchi, MD, PhD; Shigeru Kinoshita, MD, PhD

ABSTRACT

PURPOSE: To evaluate clinical outcomes of the limbal relaxing incision (LRI) combined with bimanual phacoemulsification and insertion of an intraocular lens (IOL) developed for bimanual microincision cataract surgery (MICS).

METHODS: In a prospective, single-center study, eyes with ≥0.75 diopters (D) of keratometric astigmatism were randomly assigned to two surgical techniques: 1) bimanual MICS (non-LRI group) or 2) LRI combined with bimanual MICS (LRI group). Postoperative uncorrected distance visual acuity (UDVA), corrected distance visual acuity (CDVA), postoperative refractive error, corneal topography, and vector analysis of keratometric change between pre- and postoperative eyes were compared.

RESULTS: In all cases of astigmatism in the LRI group, incisions for phacoemulsification and IOL insertion did not overlap or affect the LRIs. Uncorrected distance visual acuity was significantly higher in the LRI group (mean: 0.94), than in the non-LRI group (mean: 0.71, $P=.009$), although no difference was seen in CDVA in either group. Postoperative cylindrical error was significantly lower in the LRI group than in the non-LRI group (0.56 D and 1.51 D, respectively, $P=.0004$). Cravy analysis showed that the vector change in cylinder was 1.44 D in the LRI group and 0.18 D in the non-LRI group ($P=.0007$).

CONCLUSIONS: Limbal relaxing incision with bimanual MICS is an easy-to-follow combined surgery to correct preexisting astigmatism with predictable accuracy. [*J Refract Surg.* 2009;xx:xxx-xxx.]

doi:10.3928/1081597X-

The limbal relaxing incision (LRI) is known to be a useful and convenient procedure for reducing astigmatism, especially after cataract surgery.[1,2] In this procedure, a pair of arc-shaped corneal incisions, 400 to 550 µm in depth, are made in the steep axis inside the surgical limbus, with the incision angle determined by the degree of astigmatism.[3] The LRI flattens the corneal sphere in the steep axis to decrease corneal refractive power. This procedure does not require an extensive amount of equipment capital investment and it can also be performed during cataract surgery to correct preexisting astigmatism,[2] thus resulting in an enhanced outcome for cataract surgery. However, conventional cataract removal and intraocular lens (IOL) implantation create astigmatism at various degrees and reduce the accuracy of astigmatism correction. Moreover, the phacoemulsification incision and LRI sometimes mutually interfere, depending on the astigmatism angle, because LRI involves one pair of 40° to 120° arc-shaped incisions at various angles, which can make combined surgery more technically difficult due to a reduction in corneal rigidity.

On the other hand, bimanual microincision cataract surgery (MICS) can be performed through a 0.9-mm incision using a 22-gauge phacoemulsification needle and a 22-gauge irrigating chopper,[4] and the newly developed Y-60H MICS IOL (Hoya Corp, Tokyo, Japan) can be inserted through a 1.6-mm incision.[5] We report the clinical results of LRI combined with a 0.9-mm incision bimanual phacoemulsification and implantation of the Hoya Y-60H MICS IOL.

PATIENTS AND METHODS

A prospective study was conducted in a single center between September 2007 and July 2008. Patients were ran-

From Ouchi Eye Clinic (Ouchi); and the Department of Ophthalmology, Kyoto Prefectural University of Medicine (Ouchi, Kinoshita), Kyoto, Japan.

The authors have no proprietary or financial interest in the materials presented herein.

Correspondence: Masayuki Ouchi, MD, PhD, Ouchi Eye Clinic, 47-1 Karahashi Rajomon-cho, Minami-ku, Kyoto 601-8453, Japan. Tel: 81 75 662 7117; Fax: 81 75 662 7118; E-mail: mouchi@skyblue.ocn.ne.jp

Received: February 6, 2009; Accepted: August 13, 2009

TABLE 1

Baseline Parameters for the Limbal Relaxing Incision (LRI) and Non-LRI Groups

Parameter	LRI Group	Non-LRI Group	*P* Value
Number of eyes	96	93	
Men:women	32:45	32:48	
Right eyes:left eyes	53:43	51:42	
Mean age±SD (range) (y)	70.8±7.9 (55 to 82)	63.7±8.2 (48 to 87)	
Mean spherical equivalent±SD (range) (D)	0.12±4.46 (−12.50 to 4.25)	0.68±3.10 (−5.25 to 3.50)	.33
Preoperative cylinder±SD (range) (D)	1.79±1.01 (0.75 to 3.00)	1.65±0.65 (0.75 to 3.00)	.68
UDVA±SD (range)	0.35±0.19	0.47±0.20	.54
CDVA±SD (range	0.51±0.48	0.58±0.56	.44

UDVA=uncorrected distance visual acuity (decimal converted from logMAR), CDVA= corrected distance visual acuity (decimal converted from logMAR)
LRI group denotes patients who underwent bimanual microincision cataract surgery with LRI.
Non-LRI group denotes patients who underwent bimanual microincision cataract surgery without LRI.
Note: Data for 3 of 192 patients were not included due to perioperative complications.

TABLE 2

Fukuyama's Nomogram for Limbal Relaxing Incision (LRI) to Correct Astigmatism With Phacoemulsification

	Arc to be Incised (°)	
Cylinder (D)	Against-the-Rule and Oblique Astigmatism	With-the-Rule Astigmatism
0.75	30	60
1.00	45	70
1.50	60	80
2.00	75	90
≥3.00	90	110

Age (y)	LRI Incision Depth
Under 70	90% of central corneal thickness
70 to 80	85% of central corneal thickness
Over 80	80% of central corneal thickness

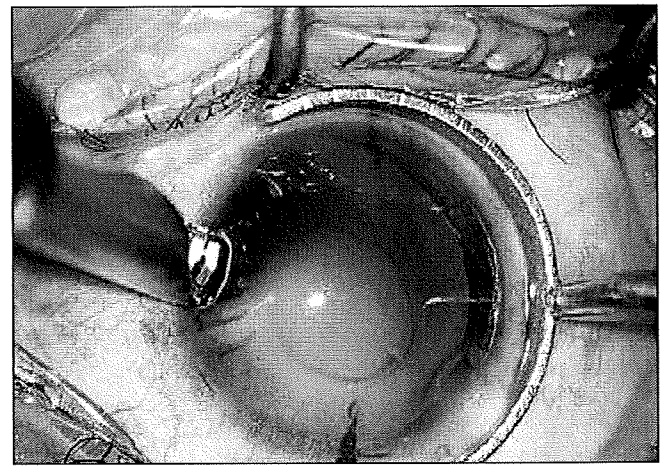

Figure 1. The limbal relaxing incision after lens extraction by 0.9-mm bimanual phacoemulsification.

domized by placing the patients' ID number in an envelope. The study population consisted of 192 eyes of 157 patients with ≥0.75 diopters (D) of keratometric astigmatism in the healthy cornea and a corticonuclear cataract of grade 3 to 4. Patient age ranged from 48 to 87 years (mean: 67.2 years). All procedures were approved by the ethics committee of Ouchi Eye Clinic, and the study was conducted in accordance with the tenets of the Declaration of Helsinki. All operations were performed by the same surgeon (M.O.).

After obtaining informed consent, the patients were randomly assigned to two groups. Ninety-six eyes of 77 patients received LRI combined with bimanual MICS (LRI group) and 93 eyes of 80 patients received only bimanual MICS (non-LRI group). Baseline characteristics for the two groups are summarized in Table 1. Exclusion criteria included perioperative complications such as failure to place the IOL in the capsular bag, suturing of the wound, and any complication necessitating enlargement of the incision or insertion of another IOL. All patients were examined preoperatively and 6 months postoperatively. Zernike harmonic analysis of the topography data was used to measure the corneal regular astigmatism in the central 3-mm area obtained

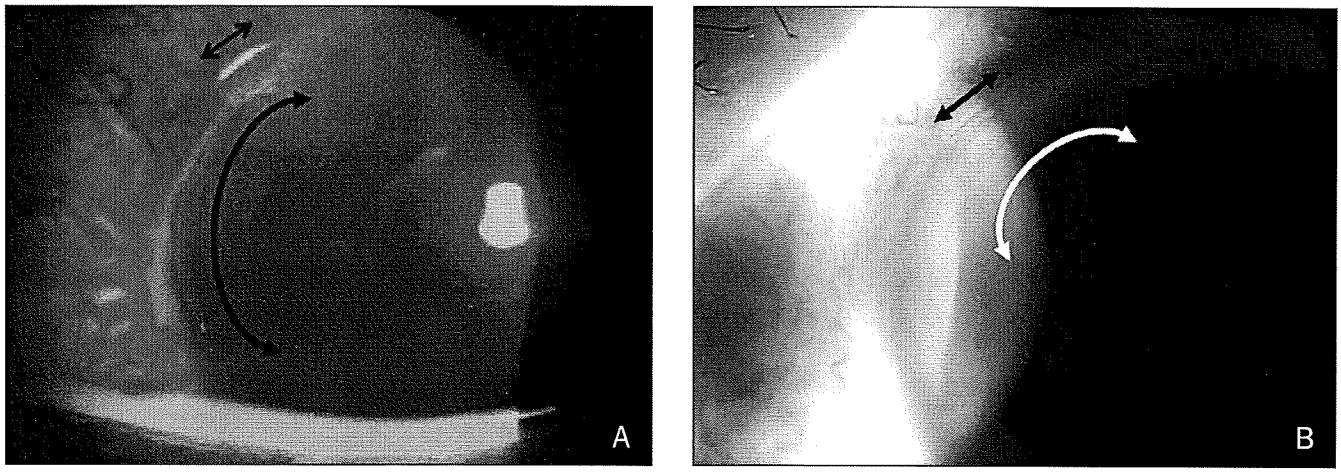

Figure 2. Postoperative examination of the 0.9-mm incision for phacoemulsification (arrowhead line) and limbal relaxing incision (arc line) do not mutually interact, even in the case of **A)** against-the-rule astigmatism or **B)** oblique astigmatism.

TABLE 3

Mean Postoperative Results for the Limbal Relaxing Incision (LRI) and Non-LRI Groups

	Mean±Standard Deviation (Range)		
Parameter	**LRI Group**	**Non-LRI Group**	***P* Value**
UDVA	0.94±0.34 (0.4 to 1.5)	0.71±0.52 (0.08 to 1.5)	.009
CDVA	1.12±0.30 (0.6 to 1.5)	1.18±0.31 (0.5 to 1.5)	.53
Spherical equivalent refraction in CDVA	0.50±0.35 (−1.5 to 1.5)	0.21±0.74 (−1.5 to 1.5)	.33
Cylindrical refraction in CDVA	0.56±0.87 (0 to 1.75)	1.51±0.79 (0.75 to 3.0)	.0004

UDVA=uncorrected distance visual acuity (decimal converted from logMAR), CDVA= corrected distance visual acuity (decimal converted from logMAR)
LRI group denotes patients who underwent LRI combined with bimanual microincision cataract surgery.
Non-LRI group denotes patients who underwent bimanual microincision cataract surgery without LRI.

with OPD-Scan II (NIDEK Co Ltd, Gamagori, Japan) and the Cravy vector analysis formula was used for evaluation of the results.[6] Postoperative uncorrected distance visual acuity (UDVA), corrected distance visual acuity (CDVA), and mean spherical equivalent and cylindrical refraction were also evaluated.

SURGICAL TECHNIQUE

Prior to surgery, three marks (two horizontal and one vertical) were made along the limbus using a 24-gauge needle with marker ink (Gentian Violet Marker Pad; BD [Becton, Dickinson and Co], Franklin Lakes, NJ) with the patient in a sitting position. Next, two 0.9-mm corneal incisions were made; one incision each at the 10- and 2-o'clock positions using a 0.9-mm MVR knife (EdgeAhead Stiletto, BD). A viscoelastic agent was injected via one of the incisions and continuous curvature capsulorrhexis was performed using a 26-gauge needle. Gentle hydrodissection and delineation was performed, followed by bimanual phacoemulsification using a 22-gauge phacoemulsification needle and an Agarwal 22-gauge irrigating chopper (MST, Redmond, Wash) through the 0.9-mm corneal incision. Bimanual cortex aspiration was then performed via the 0.9-mm corneal incision. After the capsule was filled with the viscoelastic agent, the steepest meridian was marked with a Fukuyama LRI 60° marker (ASICO, Westmont, Ill) at the peripheral cornea according to the corneal topography. The eyeball was fixed with a fixation ring, and the corneal limbus was incised using a diamond LRI knife (ASICO) at a preplanned angle depending on the degree of astigmatism and patient age-dictated Fukuyama's nomogram (Table 2, Fig 1). Preoperatively, central corneal thickness was measured using the AL-2000 biometer/pachymeter (Tomey Corp, Nagoya, Japan), and incision depth was determined based on central corneal thickness and patient age. If the patient was under 70 years old, the LRI incision depth was 90% of the central corneal thickness; 85% was used when patient age was between 70 and 80 years. If the patient was >80 years, the LRI incision depth was 80% of the central corneal thickness.

Even under strong pressure, the viscoelastic agent did not leak out though the 0.9-mm clear corneal incision and corneal distortion never occurred. The LRI in this surgical method can be performed as easily as LRI performed independently due to the excellent stability of the cornea, even after a lensectomy. In this tech-

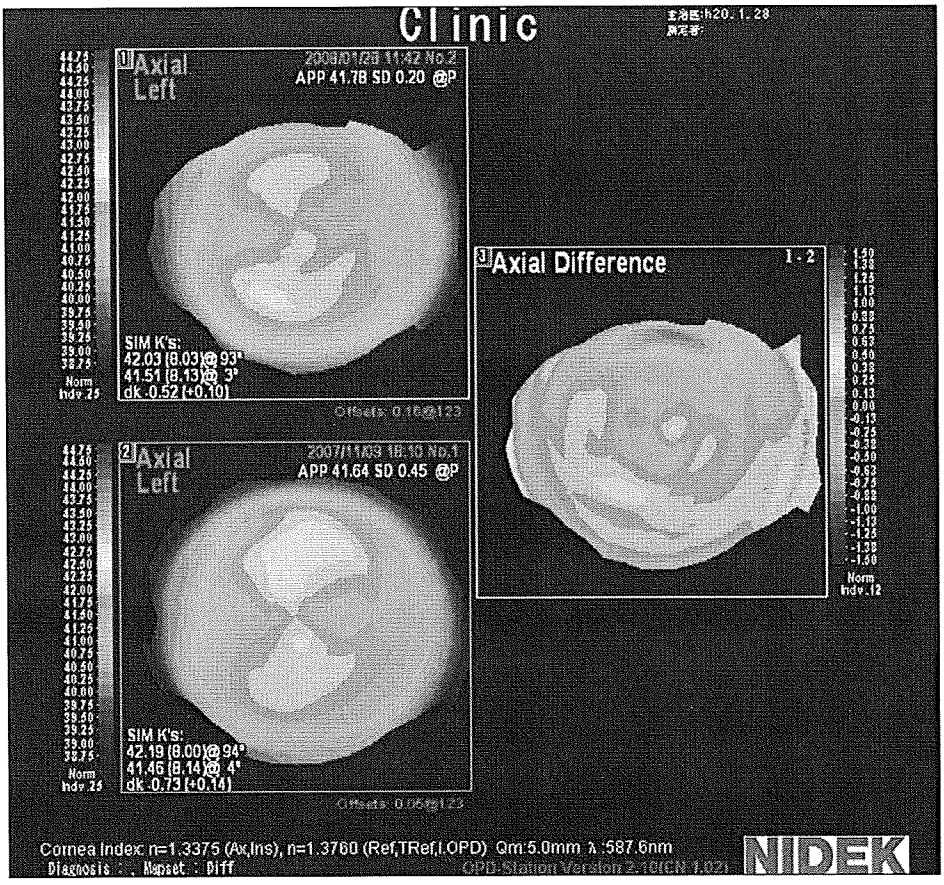

Figure 3. Corneal topography of a non-limbal relaxing incision case shows no change from **lower left)** preoperative to **upper left)** 3-month postoperative, and **right)** axial difference maps.

nique, a 0.9-mm phacoemulsification incision is made at the limbus and LRIs are made at 1 mm inside the limbus. After making one pair of LRIs, a new 1.6-mm clear corneal incision was made at an area of the cornea that was away from, and did not affect, the pair of arc-shaped LRIs. The IOL was inserted via the superior site in the case of against-the-rule astigmatism and in non-LRI cases, via the temporal site in the case of with-the-rule astigmatism, and via enlarged paracentesis in oblique astigmatism.

The Hoya Y-60H IOL was then inserted through the new 1.6-mm corneal incision.[5]

Statistical Analysis

Differences in all data were assessed using a 2-sided paired *t* test. A *P* value <.05 was considered statistically significant.

RESULTS

Of the 192 eyes initially enrolled in the study, 3 were excluded due to perioperative complications (2 due to failure to place the IOL in the bag and 1 due to posterior capsule rupture, necessitating the insertion of another IOL and wound suturing). No case of delayed or irregular healing associated with the LRI/cataract combined surgery was noted. In all cases of astigmatism, incisions for phacoemulsification and IOL insertion did not overlap or affect the LRIs (Fig 2). No significant difference between the two groups in preoperative UDVA (decimal converted from logMAR), CDVA (decimal converted from logMAR), and cylindrical refraction (Table 1) was noted. Table 3 shows mean postoperative UDVA, CDVA, spherical equivalent refraction, and cylindrical refraction. The LRI group registered significantly higher UDVA due to small postoperative corneal astigmatism, although no difference was seen in postoperative CDVA. The non-LRI group eyes showed small corneal topography changes between the pre- and postoperative periods; a typical case is shown in Figure 3. The Cravy vector analysis formula showed that the mean change of corneal regular astigmatism was 0.18±0.13 D (range: 0.07 to 0.46) postoperatively. On the other hand, there was a marked corneal change in the LRI group eyes (Fig 4) and the mean change of corneal regular astigmatism was 1.44±0.79 D (range: 0.20 to 3.45) (*P*=.0007). The pre- and postoperative corneal topography of a typical LRI-group eye is shown in Figure 4. A typical "bowtie pattern" was seen in preoperative topography but disappeared in postoperative topography.

DISCUSSION

Limbal relaxing incision/cataract combined surgery was first reported in 1998.[7] This procedure is now widely accepted by cataract surgeons due to its simplicity and relatively low investment required to purchase the associated surgical equipment compared with that needed for LASIK. Compared to astigmatic keratotomy,[8] LRI/cataract combined surgery has a low percentage of complications such as corneal perfora-

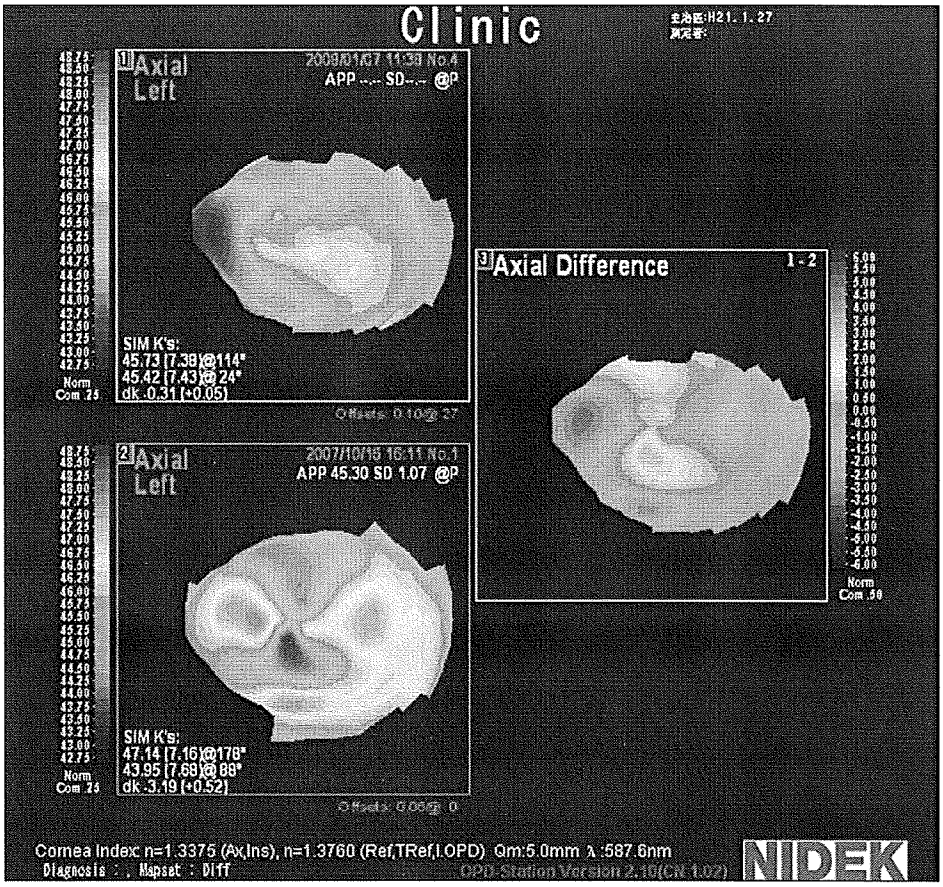

Figure 4. Corneal topography of a limbal relaxing incision case. **Lower left)** Preoperative topography map shows the typical bowtie pattern, but the **upper left)** 3-month postoperative map does not. **Right)** Axial difference map.

tion, axis shifts, or overcorrection. Moreover, the LRI does not affect intraocular visibility during cataract surgery as the incisions are made at the peripheral cornea. However, the effect of cataract surgery on postoperative astigmatism cannot be ignored entirely, even in conventional small-incision surgery, and it has been shown that the smaller surgical incision results in less postoperative astigmatism and corneal higher order aberrations.[9-11] Moreover, in the case of with-the-rule astigmatism, the superior incision used for cataract surgery sometimes affects the LRI, and in the case of against-the-rule astigmatism, the temporal corneal incision overlaps the LRI.

On the other hand, bimanual phacoemulsification using a 22-gauge instrument needs only a 0.9-mm corneal incision.[4] In addition, insertion of the IOL is accomplished via the 1.6-mm clear corneal incision,[5] an incision size small enough to enable surgeons to choose the most appropriate wound position independent of the phacoemulsification incision. With this technique, surgeons can insert the IOL far from the LRI in all cases and angles of astigmatism. This procedure thereby avoids affecting the corneal axis and construction of the LRI. Moreover, the topography and Cravy analysis performed in this study showed that the bimanual MICS with a 22-gauge instrument and MICS IOL insertion had little or no effect on keratometric change. This means that the combined LRI effect directly reflects the postoperative astigmatic change and can be performed with good predictable accuracy that is also due to the use of improved LRI nomograms such as the Nichamin nomogram.[3]

Limbal relaxing incision combined with 0.9-mm bimanual phacoemulsification and MICS IOL implantation is a useful procedure that can achieve accurate correction of preexisting astigmatism leading to good UDVA after cataract surgery.

AUTHOR CONTRIBUTIONS

Study concept and design (M.O., S.K.); data collection (M.O.); analysis and interpretation of data (M.O.); drafting of the manuscript (M.O.); critical revision of the manuscript (S.K.); statistical expertise (M.O.); administrative, technical, or material support (S.K.)

REFERENCES

1. Nichamin LD. Astigmatism control. *Ophthalmol Clin North Am.* 2006;19:485-493.
2. Müller-Jensen K, Fischer P, Siepe U. Limbal relaxing incisions

to correct astigmatism in clear corneal cataract surgery. *J Refract Surg.* 1999;15:586-589.

3. Nichamin LD. Nomogram for limbal relaxing incisions. *J Cataract Refract Surg.* 2006;32:1408.
4. Agarwal A, Agarwal A, Agarwal S, Narang P, Narang S. Phakonit: phacoemulsification through a 0.9 mm corneal incision. *J Cataract Refract Surg.* 2001;27:1548-1552.
5. Ouchi M. Using the HOYA Y-60H intraocular lens for micro-incision cataract surgery: early clinical results. *Japanese Journal of Cataract and Refractive Surgery.* 2008;22:67-72.
6. Cravy TV. Calculation of the change in corneal astigmatism following cataract extraction. *Ophthalmic Surg.* 1979;10:38-49.
7. Budak K, Friedman NJ, Koch DD. Limbal relaxing incisions with cataract surgery. *J Cataract Refract Surg.* 1998;24:503-508.
8. Oshika T, Shimazaki Y, Yoshitomi F, Oki K, Sakabe I, Matsuda S, Shiwa T, Fukuyama M, Hara Y. Arcuate keratotomy to treat corneal astigmatism after cataract surgery: a prospective evaluation of predictability and effectiveness. *Ophthalmology.* 1998;105:2012-2016.
9. Shepherd JR. Induced astigmatism in small incision cataract surgery. *J Cataract Refract Surg.* 1989;15:85-88.
10. Hayashi K, Yoshida M, Hayashi H. Postoperative corneal shape changes: microincision versus small-incision coaxial cataract surgery. *J Cataract Refract Surg.* 2009;35:233-239.
11. Yao K, Tang X, Ye P. Corneal astigmatism, high order aberrations, and optical quality after cataract surgery: microincision versus small incision. *J Refract Surg.* 2006;22:S1079-S1082.

AUTHOR QUERIES

Patients and Methods method of randomization was changed. Okay as edited?

Table 1, please provide range for UDVA and CDVA.

The mean and range of follow-up indicated in your reply to queries states 11.2 months (6 to 16 month), however, page 2 right column indicated follow-up was 6 months postoperative. Please clarify.

Table 3, please confirm range of Spherical Equivalent Refraction in CDVA as shown. Is it the same for both groups?

QUERIES PER DR WARING

Please indicate clearly in Methods, and in your nomogram table, that you are using a pair of incisions, and not just a single incision.

Is the 1998 Budak reference really the first description of limbal relaxing incisions with cataract surgery? As you know, transverse keratotomy is about 130 years old. I would be surprised if someone had not used transverse keratotomy with cataract surgery before 1998. Maybe you mean simultaneous surgery using limbal relaxing incisions only as opposed to other forms of transverse keratotomy not done simultaneously. Please clarify this in the Discussion text.

In your Discussion, please mention toric intraocular lenses as an alternative. I fully understand that you cannot include a detailed discussion of all methods of astigmatism correction, but I think you should at least briefly mention the role of toric IOLs as the most commonly used alternative to astigmatism correction with LRIs.

Functional Role of Thymic Stromal Lymphopoietin in Chronic Allergic Keratoconjunctivitis

Akira Matsuda,[1,2] *Nobuyuki Ebihara,*[1] *Norihiko Yokoi,*[2] *Satoshi Kawasaki,*[2] *Hidetoshi Tanioka,*[2] *Tsutomu Inatomi,*[2] *Rene de Waal Malefyt,*[3] *Junji Hamuro,*[2] *Shigeru Kinoshita,*[2] *and Akira Murakami*[1]

Purpose. Previous reports have shown that thymic stromal lymphopoietin (TSLP) plays a role in atopic diseases. This study was undertaken to investigate the expression of TSLP in the giant papillae obtained from patients with vernal keratoconjunctivitis (VKC) or atopic keratoconjunctivitis (AKC), and its functional roles were analyzed.

Methods. TSLP mRNA expression was examined in resected conjunctival samples obtained from four patients with VKC/AKC and three control subjects by reverse transcription-polymerase chain reaction. Anti-TSLP, anti-dendritic cell-limbic system-associated membrane protein (anti-DC-LAMP), and anti-tryptase immunohistochemical staining was performed with 10 resected giant papillae. Human conjunctival epithelial (HCJE) cells were stimulated with poly I:C, with and without endosomal inhibitor, to examine TSLP mRNA expression. Cultured human mast cells were stimulated with recombinant (r)TSLP to analyze the downstream effect of TSLP.

Results. All four VKC/AKC samples showed TSLP mRNA expression; however, no TSLP mRNA expression was found in the control conjunctivae. Anti-TSLP immunohistochemical staining showed preferential expression in the epithelial cells and some infiltrated cells of the giant papillae, but not in the control conjunctivae. Double immunohistochemical staining with TSLP and DC-LAMP or tryptase showed the existence of activated dendritic cells and mast cells near TSLP-positive cells in the giant papillae. Real-time PCR analysis showed that poly I:C induced TSLP mRNA expression in HCJEs in an endosomal-function-dependent manner and that rTSLP could induce IL-13 mRNA expression in the mast cells synergistically with IL-33.

Conclusions. The TSLP protein produced in conjunctival epithelial cells plays a role in severe ocular allergy through the activation of dendritic cells and mast cells in synergy with other cytokines. (*Invest Ophthalmol Vis Sci.* 2010;51:151-155) DOI:10.1167/iovs.09-4183

From the [1]Department of Ophthalmology, Juntendo University School of Medicine, Tokyo, Japan; the [2]Department of Ophthalmology, Kyoto Prefectural University of Medicine, Kyoto, Japan; and the [3]Department of Immunology, Schering-Plough Biopharma, Palo Alto, California.

Supported by Grants-in-Aid 19659454 (SK) and 18604009 and 21592239 (AM) from MEXT (Ministry of Education, Culture, Sports, Science, and Technology) Japan.

Submitted for publication June 19, 2009; revised August 7, 2009; accepted August 11, 2009.

Disclosure: **A. Matsuda**, None; **N. Ebihara**, None; **N. Yokoi**, None; **S. Kawasaki**, None; **H. Tanioka**, None; **T. Inatomi**, None; **R. de Waal Malefyt**, Schering-Plough Biopharma (E); **J. Hamuro**, None; **S. Kinoshita**, None; **A. Murakami**, None

Corresponding author: Akira Matsuda, Department of Ophthalmology, Juntendo University School of Medicine, 2-1-1, Hongo, Bunkyo-Ku, Tokyo, 113-8431, Japan; akimatsu@juntendo.ac.jp.

Both vernal keratoconjunctivitis (VKC)[1] and atopic keratoconjunctivitis (AKC)[2] are types of severe chronic allergic conjunctivitis in which giant papillae formation is frequently observed. In the acute stage, there is massive local infiltration by mast cells, T helper 2 (Th2) cells, and eosinophils, and there is Th2 cytokine expression. Recently, the roles of thymic stromal lymphopoietin (TSLP), an IL-7-like cytokine, were investigated in atopic diseases (e.g., atopic dermatitis and atopic asthma) because of its specific expression in the epithelium in the presence of atopic diseases and its ability to activate $CD11c^+$ dendritic cells (DCs), resulting in Th2 cell priming by the DCs.[3,4] In this study, we examined the expression of TSLP mRNA and protein using in vivo samples obtained from the resected giant papillae for therapeutic purposes. We also examined the existence of activated DCs by immunohistochemical methods.

On the other hand, it has been reported that proinflammatory stimuli including synthetic double-strand RNA (poly I:C) could induce TSLP expression in various epithelial cells, including bronchial epithelial cells,[5] keratinocytes,[6] and corneal epithelial cells.[7] Stimulation with poly I:C, which is considered to be mimicking the viral infection cascade, has some clinical relevance, because other studies have reported that children who have had respiratory syncytial virus (RSV) infection are more likely to develop bronchial asthma with IgE production.[8,9] Therefore, we evaluated the effect of poly I:C-mediated signals of TSLP mRNA induction, using the human conjunctival epithelial (HCJE) cell line,[10] and tried to inhibit poly I:C-induced TSLP expression using the endosomal inhibitor bafilomycin A for the purpose of possible therapeutic intervention. In addition, we examined the downstream effect of TSLP in human cultured mast cells in synergy with another Th2 cytokine, IL-33,[11,12] to elucidate the possible role of TSLP in the pathophysiology of severe chronic allergic conjunctivitis.

Material and Methods

Giant Papillae and Control Conjunctivae Samples

Giant papillae were resected for therapeutic purposes from four patients, three with AKC and one with VKC, and control conjunctivae tissue was biopsied from patients with cataract, pterygium, or melanoma during surgery after written informed consent was obtained for TSLP mRNA analysis (Table 1). Additional giant papillae samples were obtained from six patients with AKC and four with VKC for TSLP immunostaining analysis (Table 2). All procedures were approved by the ethics committees of Juntendo University School of Medicine and Kyoto Prefectural University of Medicine, and the study was conducted in accordance with the tenets of the Declaration of Helsinki. AKC was defined as a bilateral chronic inflammation of the conjunctiva and lids associated with atopic dermatitis, and VKC was defined as a chronic, bilateral, conjunctival inflammatory condition found in individuals predisposed by their atopic background; detailed information about pa-

TABLE 1. Clinical Information for RT PCR Analysis

Sample No.	Sex	Age	Diagnosis	Total IgE
1	M	21	AKC	4263
2	M	18	AKC	5218
3	M	12	VKC	92
4	M	32	AKC	1983
5	F	72	Cataract	ND
6	M	52	Pterygium	ND

tient selection was described elsewhere.[13] Upper bulbar conjunctivae resected from six patients with conjunctivochalasis were used as control samples, as previously described,[13] after informed consent was obtained (Table 3).

Antibodies, Reagents, and Cell Lines

We purchased mouse anti-DC-LAMP (CD208) monoclonal antibody from Beckman Coulter Japan (Tokyo, Japan), mouse anti-human tryptase antibody from Dako Japan (Kyoto, Japan), and Alexa-488-conjugated donkey anti-rat IgG and Alexa-594-conjugated donkey anti-mouse IgG antibodies from Invitrogen Japan (Tokyo, Japan). Rat anti-human TSLP monoclonal antibody was prepared as previously described.[4] HCJE was kindly provided by Ilene K. Gipson (Schepens Eye Research Institute, Philadelphia, PA) and maintained with defined keratinocyte serum-free medium (KSFM; Invitrogen Japan). The human mast cell line LAD2 was kindly provided by Arnold Kirshenbaum (National Institutes of Health, Bethesda, MD), and maintained as previously described.[14] Recombinant human (r)TSLP and recombinant human (r)IL-33 were obtained from Peprotech (London, UK), poly I:C was obtained from InvivoGen (San Diego, CA), and bafilomycin A1 was obtained from Sigma-Aldrich (St. Louis, MO).

Reverse-Transcription–Polymerase Chain Reaction

Total RNA was extracted from the giant papillae tissue (NucleoSpin II RNA isolation kit; Macherey-Nagel GmbH & Co., Duren, Germany), and cDNAs were prepared from 1 μg of total RNA by using random primers and reverse transcriptase (Superscript II; Invitrogen) according to the manufacturer's protocol. PCR primers for TSLP amplification were 5′-aacaagtgtcacaattacaag-3′ (forward) and 5′-aatgtcccttagaaaagtatg-3′ (reverse), which are designed for amplifying the common region of TSLP transcript variants 1 and 2 (GenBank accession numbers: NM_033035.4 and NM_138551.3, respectively; 849-bp length; http://www.ncbi.nlm.nih.gov/Genbank; provided in the public domain by the National Center for Biotechnology Information, Bethesda, MD). PCR reaction was performed as follows: initial denaturation at 94°C for 5 minutes and at 94°C for 1 minute, annealing at 60°C for 1 minute, and extension at 72°C for 1 minute (35 cycles). IL-4[15] and IL-13[16] amplification was performed according to previously published methods, with the following pairs of primers: IL-4: 5′-ctcacagagcagaagactctgtg-caccgag-3′(forward), and 5′-cacaggacaggaattcaagcccgccaggcc-3′ (reverse); and IL-13: 5′-ccacggtcattgctctctcacttgcc-3′ (forward), 5′-ccttgt-gcgggcagaatccgctca-3′ (reverse).

TABLE 3. Summary of TSLP Immunostaining of Control Conjunctivae

Sample No.	Age	Sex	Diagnosis	TSLP	
				Epithelium	Substantia propria
1	70	F	Conjunctivochalasis	−	−
2	65	M	Conjunctivochalasis	−	−
3	71	F	Conjunctivochalasis	−	−
4	74	M	Conjunctivochalasis	−	−
5	53	F	Conjunctivochalasis	−	−
6	75	F	Conjunctivochalasis	−	−

−, negative immunostaining.

Immunohistochemistry

Giant papillae were frozen in OCT compound, and cryostat sections were then cut, mounted on slides, and fixed in 4% paraformaldehyde in PBS. Nonspecific staining was blocked (30 minutes) with blocking buffer (10% normal donkey serum, 1% bovine serum albumin [BSA] in PBS). Anti-TSLP monoclonal antibody (10 μg/mL) was then applied and reacted overnight at 4°C. After they were washed with PBS, the slides were incubated for 30 minutes with Alexa 488-conjugated anti-rat IgG. Double immunohistochemical staining was performed with pairs of anti-TSLP and anti-tryptase antibodies and anti-TSLP and anti-CD208 antibodies. The pair of primary antibodies was applied to the samples simultaneously, and the secondary antibodies (Alexa 488 anti-rat IgG and Alexa and 594 anti-mouse IgG antibodies) were then applied after the samples were washed with PBS.

HCJE Stimulation with Poly I:C and the Effect of Bafilomycin A for Poly I:C Stimulation

HCJE cells were grown in 12-well dishes and used in the subconfluent state. Poly I:C (5 μg/mL) was added to HCJE cells and incubated for 1, 3, and 8 hours in a CO_2 incubator. Simultaneously, 10 nM bafilomycin A was added to some wells to inhibit endosomal functions in the HCJE cells.

Mast Cell Stimulation with rTSLP/rIL-33 and Downstream Signal Analysis

LAD2 cells (2×10^4 cells per well in a 24-well dish) were stimulated with rTSLP (10 ng/mL) for 1, 3, and 16 hours. rIL-33 (10 ng/mL) was

TABLE 2. Summary of TSLP Immunostaining of Giant Papillae

Sample No.	Age	Sex	Total IgE	Specific IgE	Diagnosis	TSLP	
						Epithelium	Substantia Propria
1	16	F	509	positive	VKC	++	+
2	22	M	89	positive	VKC	+	+
3	13	M	2319	positive	VKC	++	++
4	18	M	375	positive	AKC	+	+
5	17	M	17260	positive	AKC	+	++
6	21	M	1904	positive	AKC	+	+
7	16	M	3763	positive	AKC	+/−	+
8	19	M	124	negative	VKC	+/−	+
9	34	M	22800	positive	AKC	+	++
10	45	F	28	negative	AKC	+	+

++, prominent immunostaining; +, positive immunostaining; +/−, sporadic immunostaining.

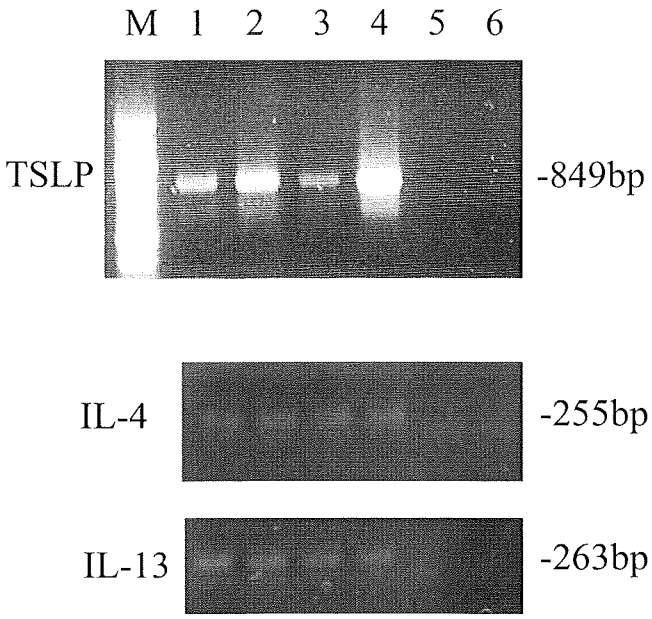

FIGURE 1. RT-PCR analysis of TSLP, IL-4, and IL-13 mRNA expression in human conjunctival tissue. RT-PCR was performed with cDNA prepared from giant papillae (*lanes1-4*) and control conjunctivae (*lanes 5, 6*). M, DNA size markers. Single bands were observed at the predicted length (849 bp for TSLP, 255 bp for IL-4, and 263 bp for IL-13) of the PCR products (*lanes 1-4*).

added alone or simultaneously to LAD2 cells. IL-13 mRNA expression in LAD2 cells was quantified by real-time PCR.

Real-Time PCR Analysis of TSLP and IL-33 mRNA Expression

Total RNA was extracted from HCJE and LAD2 cells and cDNAs were prepared from 1 μg of total RNA by using random primers as just described. We used real-time PCR probes (*Taq*Man; Applied Biosystems [ABI], Foster City, CA) and primers specific for human TSLP (Hs01572934_g1), human IL-13 (Hs00174379_m1), and 18SrRNA (Assay-on-Demand gene expression products; ABI). Real-time PCR analysis was performed on a sequence-detection system (Prism 7300; ABI). The expression of TSLP in the HCJE cells was quantified by the standard curve method, by using 18SrRNA expression in the same cDNA as a control. We calculated a standard curve with full-length human TSLP cDNA obtained by PCR reaction and subcloned into pCRII dual promoter plasmid (Invitrogen). For IL-13 mRNA expression, the comparative Ct method was used, which utilizes 18SrRNA expression in the same cDNA as a control.

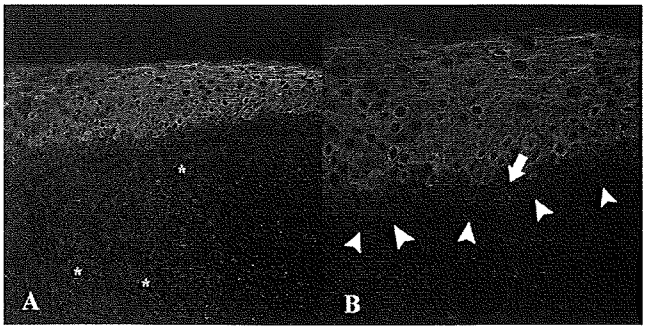

FIGURE 3. TSLP/tryptase double-immunohistochemical staining of giant papillae. Positive TSLP staining (*green*) was observed in the suprabasal-apical layers of conjunctival epithelium (**A**). Tryptase-positive mast cells (*red*) were observed underneath the epithelium, a few mast cells are also positive for TSLP (✱). (**B**) Tryptase-positive mast cells were observed around the basal cell layer of the epithelium (*arrow*) and beneath the epithelium. *Arrowheads*: the boundary between the epithelium and substantia propria. Original magnification: (**A**) ×200; (**B**) ×400.

RESULTS

RT-PCR Analysis of Giant Papillae Obtained from Patients with VKC/AKC

Total RNA was extracted from the giant papillae and control conjunctivae tissue, then RT-PCR was performed. TSLP mRNA expression was detected for all the giant papillae samples (Fig. 1, lanes 1-4); however, no TSLP mRNA expression was detected for control samples (Fig. 1, lanes 5-7).

Immunohistochemical Localization of TSLP

Anti-TSLP immunohistochemical staining was performed using giant papillae obtained from AKC/VKC patients as well as control conjunctivae. The epithelium of giant papillae showed cytoplasmic-positive immunostaining for TSLP protein (Fig. 2A). There was a clear boundary between the TSLP-positive and -negative epithelium (Fig. 2A). Additional positive TSLP staining was observed in some infiltrating cells in the giant papillae samples (Fig. 2A and 2B, asterisks). DC-LAMP-positive, activated dendritic cells were observed beneath the TSLP-positive epithelial cells and near the TSLP-positive cells in the substantia propria (Fig. 2A, arrowheads). No TSLP immunostaining was observed in the control conjunctiva sample (Fig. 2C). Double-immunostaining with anti-TSLP and anti-tryptase antibodies revealed that tryptase-positive mast cells were located beneath the TSLP-positive epithelium (Fig. 3), and some of the mast cells were found within and under the epithelium

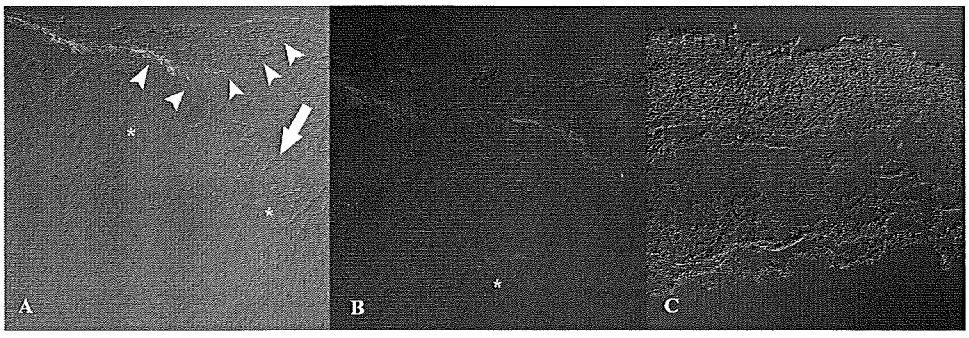

FIGURE 2. TSLP/DC-LAMP double-immunohistochemical staining of giant papillae. Cytoplasmic TSLP immunostaining (*green*) was observed in the epithelial cells of giant papillae. There is a clear boundary between the TSLP-positive- and -negative epithelium within the same section. The boundary between the epithelium and substantia propria is indicated by *arrowheads* (**A**, higher magnification in **B**). Some TSLP-positive cells were also observed at the substantia propria (*arrow*). DC-LAMP-immunopositive dendritic cells (*red*) were observed underneath the TSLP-positive conjunctival epithelium and near the TSLP-positive cells in the substantia propria (✱). No TSLP-positive staining was observed in the control conjunctiva (**C**). Original magnification: (**A**, **C**) ×200, (**B**) ×400.

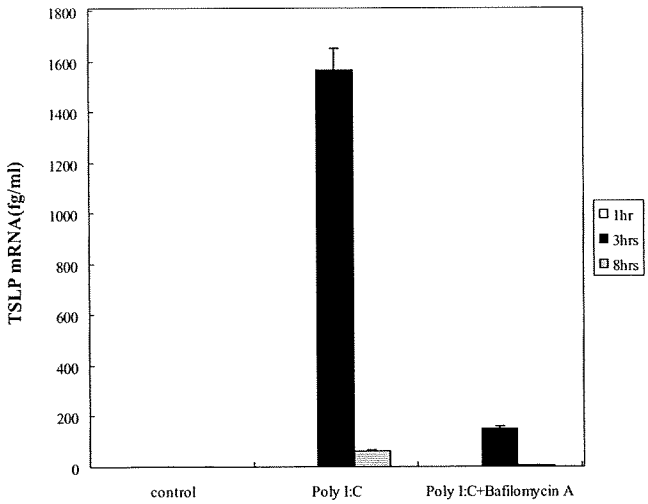

FIGURE 4. Real-time PCR analysis of TSLP mRNA expression using HCJE cells. The cells were stimulated with poly I:C (5 μg/mL) for 1, 3, and 8 hours, with or without the endosomal inhibitor bafilomycin A. cDNA was prepared from each sample, and TSLP mRNA expression was quantified by real-time PCR, with the standard curve method. Data are representative of results in three independent experiments performed in triplicate.

(Fig. 3B). A few mast cells were also positive for TSLP immunostaining (Fig. 3A, asterisks). The immunostaining results are summarized in Tables 2 and 3.

Poly I:C-Induced TSLP Expression in HCJE Cells

cDNAs were synthesized from total RNA isolated from poly I:C-stimulated HCJE cells. TSLP mRNA induction was observed in HCJE cells stimulated with poly I:C (5 μg/mL) at 3 hours after stimulation (Fig. 4). Simultaneous addition of 10 nM bafilomycin A showed inhibition of poly I:C-induced TSLP mRNA expression (Fig. 4).

TSLP-Induced IL-33 mRNA Expression in Synergy with IL-33

The human mast cell line LAD2 was stimulated with rTSLP (10 ng/mL), rIL-33 (10 ng/mL), and rTSLP+rIL-33 for 1, 3, and 16 hours. Relative IL-13 mRNA expression was quantified with real-time PCR. rTSLP alone did not induce IL-13 mRNA expression, and rIL-33 induced modest IL-13 expression (30-fold, compared with the unstimulated LAD2 cells). Co-stimulation of LAD2 cells with rTSLP and rIL-33 synergistically induced IL-13mRNA expression (150-fold) and peaked at 1 hour after co-stimulation (Fig. 5).

DISCUSSION

In this study, we detected in vivo expression of TSLP mRNA/protein in the giant papillae tissues obtained from patients with VKC/AKC, and no TSLP expression was observed in the control samples (Figs. 1, 2A, 2C). To the best of our knowledge, this is the first report of TSLP expression in an ocular surface disorder. As has been reported about other allergic diseases such as atopic dermatitis[4] and bronchial asthma,[17] preferential TSLP expression was observed in the epithelial cells of chronic allergic conjunctivitis. Restricted TSLP protein expression was clearly observed at the surface epithelial cells (Fig. 2A). This finding was also consistent with those in a previous report on atopic dermatitis.[4]

We also observed some TSLP-positive cells in the substantia propria of the giant papillae (Fig. 2, arrow). Corrigan et al.[18] recently reported that TSLP-positive neutrophils, mast cells, and macrophages were observed in the antigen-challenged dermis obtained from atopic patients. Therefore, we theorize that the TSLP-positive cells in the giant papillae may be these inflammatory cells. We found that at least some mast cells express TSLP protein (Fig. 3A, asterisks), which is consistent with previous studies that showed that the mast cells activated through the IgE receptor express TSLP mRNA.[4,19] Our double-immunohistochemistry results also showed that tryptase-positive mast cells localize in the vicinity of TSLP-positive epithelial cells in the giant papillae (Fig. 3B, arrow), and our result adds support to the proposal of Miyata et al.[20] that mast cells are essential for TSLP expression in the epithelium of the mouse allergic rhinitis model.

It is known that one of the major functions of TSLP is activating dendritic cells, which prime naïve T cells to produce the proallergic cytokines, such as IL-4, -5, and -13.[4] We therefore determined the existence of activated dendritic cells by using the dendritic cell activation marker DC-LAMP and found the existence of activated dendritic cells in the vicinity of the TSLP-positive cells (Fig. 2, asterisks). The DC-LAMP-positive dendritic cells were observed not only underneath the TSLP-positive epithelial cells but also near the TSLP-positive cells in the substantia propria (Fig. 2A, arrow). This result adds support to the recent results of Corrigan at al.,[18] who proposed a possible role of TSLP-positive inflammatory cells in the activation of dendritic cells in the dermis of atopic skin challenged with allergen.

As a next step, we examined the expression of TSLP mRNA in HCJE cells[10] with added poly I:C. As reported previously in bronchial epithelial cells[5] and corneal epithelial cells,[7] poly I:C stimulation induces TSLP mRNA expression in the conjunctival epithelial cells. We analyzed the time course of TSLP mRNA expression and found that it peaked at 3 hours after poly I:C stimulation (Fig. 4). Our results are consistent with those of Ma et al.,[7] who showed peak TSLP mRNA expression at 3 hours after stimulation of human corneal epithelial cells. We then tried to inhibit poly I:C-induced TSLP mRNA expression by the endosomal inhibitor bafilomycin. Previous reports showed that poly I:C-induced IL-6 expression in a peripheral blood mononuclear cell (PBMC) requires an acidic pH (pH5.7–6.5), and bafilomycin A could inhibit poly I:C-induced IL-6 expression by inhibiting the endosomal proton pump.[21] Our results showed that a 10 nM bafilomycin treatment blocked TSLP mRNA ex-

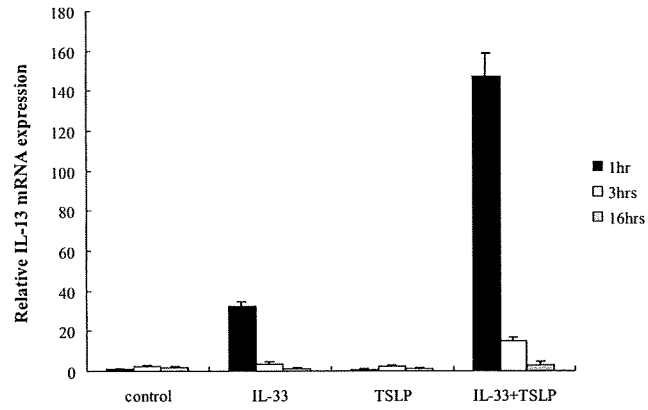

FIGURE 5. TSLP and IL-33 synergistically induced IL-13 expression in human mast cells (LAD2). The cells were stimulated with rTSLP (10 ng/mL), rIL-33 (10 ng/mL), and rTSLP+rIL-33 for 1, 3, and 16 hours. Relative IL-13 mRNA was shown to be comparable to that of unstimulated LAD2 cells obtained 1 hour after stimulation. Data are representative of results in three independent experiments performed in triplicate.

pression induced by 3-hour poly I:C stimulation (Fig. 4). We theorize that drugs that raise endosomal pH may be useful for inhibiting poly I:C-mediated TSLP expression. It is known that bafilomycin A is too toxic for clinical use; therefore, omeprazole, a proton pump inhibitor, or chloroquine, a competing basic compound that raises endosomal pH, which are widely used in the treatment of gastric ulcer and malaria, respectively, may be useful for this purpose.[22]

Finally, we examined the possible effector cells for TSLP in the chronic allergic conjunctivitis. Mast cells have been reported as one of the effector cells in TSLP signaling.[23] A previous report showed that the coculture of skin fragments from patients with atopic dermatitis (AD) with human mast cells induces TSLP protein expression and that anti-TSLP antibody treatment suppresses TSLP expression.[23] However, the authors did not perform direct stimulation of human mast cells with recombinant (r)TSLP. Therefore, we stimulated human mast cells with rTSLP and found that rTSLP treatment alone induced a minimum of IL-13 mRNA induction. A surprising finding showed that co-stimulation with another epithelial cell-derived Th2 cytokine, IL-33, had a synergistic effect for IL-13 mRNA expression in LAD2 cells (Fig. 5). In their study, Allakhverdi et al.[23] showed partial suppression of IL-13 expression using anti-TSLP antibody in a mast cell-lesional, AD-skin coculture model, so it is reasonable to consider that other skin-derived factor(s) also contribute to IL-13 mRNA expression. Very recently, we reported IL-33 protein expression in the epithelial cells of giant papillae as well as TSLP,[12] and so we considered that TSLP-IL-33 co-stimulation may play a role in the pathogenesis of chronic allergic diseases through the activation of mast cells.

In summary, we found in vivo expression of TSLP in the epithelial cells of giant papillae, and we theorize that TSLP protein may play a role in the pathogenesis of severe chronic allergic conjunctivitis through the activation of dendritic cells or mast cells in synergy with other proinflammatory cytokines such as IL-33. The double-stranded RNA molecule, associated with viral infection, may induce expression of TSLP, and the endosomal inhibitor bafilomycin may be useful for inhibiting this activation.

Acknowledgments

The authors thank Hisako Hitora-Takeshita for excellent technical support; Julian M. Hopkin for his invaluable continuous support; Ilene K. Gipson for providing the HCJE cell line; Arnold Kirshenbaum for providing the LAD2 cell line; and John Bush for editing the English.

References

1. Montan PG, Biberfeld PJ, Scheynius A. IgE, IgE receptors, and other immunocytochemical markers in atopic and nonatopic patients with vernal keratoconjunctivitis. *Ophthalmology.* 1995;102:725-732.
2. Foster CS, Rice BA, Dutt JE. Immunopathology of atopic keratoconjunctivitis. *Ophthalmology.* 1991;98:1190-1196.
3. Zhou B, Comeau MR, De Smedt T, et al. Thymic stromal lymphopoietin as a key initiator of allergic airway inflammation in mice. *Nat Immunol.* 2005;6:1047-1053.
4. Soumelis V, Reche PA, Kanzler H, et al. Human epithelial cells trigger dendritic cell mediated allergic inflammation by producing TSLP. *Nat Immunol.* 2002;3:673-680.
5. Kato A, Favoreto S Jr, Avila PC, Schleimer RP. TLR3- and Th2 cytokine-dependent production of thymic stromal lymphopoietin in human airway epithelial cells. *J Immunol.* 2007;179:1080-1087.
6. Kinoshita H, Takai T, Le TA, et al. Cytokine milieu modulates release of thymic stromal lymphopoietin from human keratinocytes stimulated with double-stranded RNA. *J Allergy Clin Immunol.* 2009;123:179-186.
7. Ma P, Bian F, Wang Z, et al. Human corneal epithelium-derived thymic stromal lymphopoietin: a potential link between the innate and adaptive immune responses via Toll-like receptors and Th2 cytokines. *Invest Ophthalmol Vis Sci.* 2009;50(6):2702-2709.
8. Welliver RC, Kaul TN, Ogra PL. The appearance of cell-bound IgE in respiratory-tract epithelium after respiratory-syncytial-virus infection. *N Engl J Med.* 1980;303:1198-1202.
9. Chen CH, Lin YT, Yang YH, et al. Ribavirin for respiratory syncytial virus bronchiolitis reduced the risk of asthma and allergen sensitization. *Pediatr Allergy Immunol.* 2008;19:166-172.
10. Gipson IK, Spurr-Michaud S, Argueso P, Tisdale A, Ng TF, Russo CL. Mucin gene expression in immortalized human corneal-limbal and conjunctival epithelial cell lines. *Invest Ophthalmol Vis Sci.* 2003;44:2496-2506.
11. Schmitz J, Owyang A, Oldham E, et al. IL-33, an interleukin-1-like cytokine that signals via the IL-1 receptor-related protein ST2 and induces T helper type 2-associated cytokines. *Immunity.* 2005;23:479-490.
12. Matsuda A, Okayama Y, Terai N, et al. The role of interleukin-33 in chronic allergic conjunctivitis. *Invest Ophthalmol Vis Sci.* Published online May 20, 2009.
13. Matsuda A, Okayama Y, Ebihara N, et al. Hyperexpression of the high-affinity IgE receptor-beta chain in chronic allergic keratoconjunctivitis. *Invest Ophthalmol Vis Sci.* 2009;50:2871-2877.
14. Kirshenbaum AS, Akin C, Wu Y, et al. Characterization of novel stem cell factor responsive human mast cell lines LAD 1 and 2 established from a patient with mast cell sarcoma/leukemia; activation following aggregation of FcepsilonRI or FcgammaRI. *Leuk Res.* 2003;27:677-682.
15. Goodman RE, Nestle F, Naidu YM, et al. Keratinocyte-derived T cell costimulation induces preferential production of IL-2 and IL-4 but not IFN-gamma. *J Immunol.* 1994;152:5189-5198.
16. Burd PR, Thompson WC, Max EE, Mills FC. Activated mast cells produce interleukin 13. *J Exp Med.* 1995;181:1373-1380.
17. Ying S, O'Connor B, Ratoff J, et al. Expression and cellular provenance of thymic stromal lymphopoietin and chemokines in patients with severe asthma and chronic obstructive pulmonary disease. *J Immunol.* 2008;181:2790-2798.
18. Corrigan CJ, Jayaratnam A, Wang Y, et al. Early production of thymic stromal lymphopoietin precedes infiltration of dendritic cells expressing its receptor in allergen-induced late phase cutaneous responses in atopic subjects. *Allergy.* 2009;64(7):1014-22.
19. Okayama Y, Okumura S, Sagara H, et al. FcepsilonRI-mediated thymic stromal lymphopoietin production by IL-4-primed human mast cells. *Eur Respir J.* 2009;34(2):425-35.
20. Miyata M, Hatsushika K, Ando T, et al. Mast cell regulation of epithelial TSLP expression plays an important role in the development of allergic rhinitis. *Eur J Immunol.* 2008;38:1487-1492.
21. de Bouteiller O, Merck E, Hasan UA, et al. Recognition of double-stranded RNA by human toll-like receptor 3 and downstream receptor signaling requires multimerization and an acidic pH. *J Biol Chem.* 2005;280:38133-38145.
22. Lee CM, Tannock IF. Inhibition of endosomal sequestration of basic anticancer drugs: influence on cytotoxicity and tissue penetration. *Br J Cancer.* 2006;94:863-869.
23. Allakhverdi Z, Comeau MR, Jessup HK, et al. Thymic stromal lymphopoietin is released by human epithelial cells in response to microbes, trauma, or inflammation and potently activates mast cells. *J Exp Med.* 2007;204:253-258.

Hyperexpression of the High-Affinity IgE Receptor-β Chain in Chronic Allergic Keratoconjunctivitis

Akira Matsuda,[1] Yoshimichi Okayama,[2] Nobuyuki Ebihara,[3] Norihiko Yokoi,[1] Junji Hamuro,[1] Andrew F. Walls,[4] Chisei Ra,[2] Julian M. Hopkin,[5] and Shigeru Kinoshita[1]

Purpose. Although the existence of FcεRI-$\alpha\beta\gamma_2$ and FcεRI-$\alpha\gamma_2$ receptor subtypes was reported, there has been no direct evidence of these two subtypes of FcεRI in vivo. To investigate the existence of these two subtypes of FcεRI in vivo, the authors evaluated the expression of FcεRI-β in the giant papillae of chronic allergic conjunctivitis and compared the expression level of FcεRI-β with control conjunctivae using the anti-human FcεRI-β antibody.

Methods. FcεRI-β expression in giant papillae obtained from patients with atopic keratoconjunctivitis and vernal keratoconjunctivitis in control conjunctivae was evaluated by immunohistochemistry using anti-FcεRI-β, -α, -γ, and anti-human mast cell tryptase, anti-chymase, anti-basophil, and anti-CD1a antibodies.

Results. Statistical analyses revealed that the densities of FcεRI-β^+ cells, FcεRI-α^+ cells, tryptase$^+$ cells, and FcεRI-β^+/tryptase$^+$ cells were significantly increased in giant papillae compared with controls. There were two types of FcεRI ($\alpha\beta\gamma_2$ and $\alpha\gamma_2$) on the mast cells of the giant papillae. The ratio of the FcεRI-β^+ cell number/FcεRI-α^+ cell number in the giant papillae (0.69 ± 0.08 [mean ± SD]) was significantly higher than that of the controls (0.07 ± 0.16). FcεRI-β/tryptase double immunostaining revealed that 81% ± 13% of tryptase$^+$ cells expressed FcεRI-β. FcεRI-β^+ cells were preferentially localized within and around epithelial tissue. The authors also found that FcεRI-β was expressed by basophils but not by FcεRI-$\alpha\gamma_2$-positive Langerhans cells in the giant papillae samples.

Conclusions. Preferential FcεRI-β expression observed in the mast cells and basophils of giant papillae suggests important roles of FcεRI-β in the pathophysiology of atopic keratoconjunctivitis and vernal keratoconjunctivitis. (*Invest Ophthalmol Vis Sci.* 2009;50:2871-2877) DOI:10.1167/iovs.08-3022

Human high-affinity IgE receptor (FcεRI) exists in two isoform, a tetramer containing the β chain FcεRI-$\alpha\beta\gamma_2$ and a trimer lacking the β chain FcεRI-$\alpha\gamma_2$, depending on cell type.[1] The FcεRI-β gene (*MS4A2*) has been recognized as an atopy-related gene, initially discovered from a genetic linkage study[2] and also from a genetic association study[3] by our group, and the functional roles of FcεRI-β protein have been investigated extensively. For example, the FcεRI-β chain mediates intracellular signaling through the immunoreceptor tyrosine-based activation motif and is phosphorylated in response to antigen cross-linking of the receptor-bound IgE.[1] The human FcεRI-β chain acts as an amplifier for mast cell activation and cell surface expression of FcεRI.[4,5] Although the existence of the FcεRI-$\alpha\beta\gamma_2$ and FcεRI-$\alpha\gamma_2$ receptor subtypes has been reported,[6] there has been no direct evidence of these two subtypes of FcεRI in vivo at the protein level. Furthermore, the precise pathophysiological roles of the FcεRI-β chain in human atopic diseases remain unclear. Recently, we raised an antibody against human FcεRI-β that was useful for the in situ detection of the FcεRI-β protein.[7]

Atopic keratoconjunctivitis (AKC)[8,9] and vernal keratoconjunctivititis (VKC)[10] are the most severe forms of chronic allergic conjunctivitis. Massive infiltration of mast cells occurs, and serum and tear IgE levels are significantly higher than in healthy controls.[8,11,12] In addition, AKC and VKC tend to form giant papillae at the upper tarsal conjunctiva.[8,10,13] We resected giant papillae for therapeutic purposes[14] and carried out histopathologic analysis with the resected tissues using our newly generated anti-FcεRI-β-specific antibody. We reported previously that IgE-bearing FcεRI-α^+ mast cells were increased in the giant papillae of patients with VKC[15]; however, the expression of FcεRI-β has yet to be evaluated. We found preferential FcεRI-β expression in the mast cells of giant papillae samples compared with those of the control conjunctivae.

Materials and Methods

Antibodies

Rabbit antiserum against unique C-terminal sequences of human FcεRI-β (CYSELEDPGEMSPPIDL) was generated and the antiserum was purified on a protein-A column, as previously described.[7] Because this antibody was raised against the C-terminal region of human FcεRI-β protein, it did not recognize the truncated form of FcεRI-β protein described previously.[16] Other antibodies used in this study included Alexa 488-conjugated-goat anti-rabbit-F(ab')$_2$ and Alexa 594-conjugated goat anti-mouse IgG-F(ab')$_2$ (Invitrogen, Carlsbad, CA), Cy5-conjugated goat anti-mouse IgG1 antibody (Southern Biotechnology, Birmingham, AL), rabbit anti-FcεRI-γ polyclonal antibody (Upstate Biotechnology, Lake Placid, NY), phycoerythrin (PE)-conjugated mouse anti-FcεRI-α monoclonal antibody (clone CRA1; e-bioscience, Tokyo, Japan), mouse anti-chymase monoclonal antibody (clone CC1; LAB Vision, Fremont, CA), mouse anti-CD1a monoclonal antibody

From the [1]Department of Ophthalmology, Kyoto Prefectural University of Medicine, Kyoto, Japan; the [2]Division of Molecular Cell Immunology and Allergology, Advanced Medical Research Center, Nihon University Graduate School of Medicine, Tokyo, Japan; the [3]Department of Ophthalmology, Juntendo University School of Medicine, Tokyo, Japan; the [4]Immunopharmacology Group, Southampton General Hospital, Southampton, United Kingdom; and the [5]Experimental Medicine Unit, University of Wales Swansea, Swansea, United Kingdom.

Supported in part by Wellcome Trust Traveling Research Fellowship 066797/Z/02/Z (AM); Grants-in-Aid for Scientific Research Programs 19659454 (SK), 18604009 (AM), and 20591195 (YO) from the Japanese Ministry of Education, Culture, Sports, Science and Technology; and the Japanese National Institute of Biomedical Innovation Program (Project ID05-24).

Submitted for publication October 29, 2008; revised November 24 and December 13 and 16, 2008; accepted March 30, 2009.

Disclosure: **A. Matsuda**, None; **Y. Okayama**, None; **N. Ebihara**, None; **N. Yokoi**, None; **J. Hamuro**, None; **A.F. Walls**, None; **C. Ra**, None; **J.M. Hopkin**, None; **S. Kinoshita**, None

The publication costs of this article were defrayed in part by page charge payment. This article must therefore be marked "*advertisement*" in accordance with 18 U.S.C. §1734 solely to indicate this fact.

Corresponding author: Akira Matsuda, Department of Ophthalmology, Kyoto Prefectural University of Medicine, Kawaramachi Hirokoji, Kamigyo-ku, Kyoto 602-0841, Japan; akimatsu@koto.kpu-m.ac.jp.

TABLE 1. Clinical Characteristics of Patients with AKC/VKC and FcεRI-β$^+$ Cell Numbers of Giant Papillae

Patient	Age (y)	Sex	Total IgE	Specific IgE	Diagnosis	FcεRI-β$^+$ Cells (mean ± SD)	Treatment
1	16	F	509	Positive	VKC	62.5 ± 20.0	Dex, CsA
2	22	M	89	Positive	VKC	53.9 ± 8.3	Dex
3	13	M	2319	Positive	VKC	20.2 ± 8.3	Dex
4	18	M	375	Positive	AKC	49.3 ± 22.0	Dex, CsA
5	17	M	17260	Positive	AKC	56.2 ± 21.2	Dex, CsA, oral steroid
6	21	M	1904	Positive	AKC	34.9 ± 18.0	Dex
7	16	M	3763	Positive	AKC	29.2 ± 17.0	Dex
8	19	M	124	Negative	VKC	49.4 ± 20.0	Dex
9	23	M	20328	Positive	AKC	78.3 ± 25.5	Dex
10	45	F	28	Negative	AKC	48.2 ± 12.0	Dex

Dex, 0.1% dexamethasone eyedrop; CsA, 0.1% cyclosporine eyedrop.

(clone O-10; Santa Cruz Biotechnology Inc., Santa Cruz, CA), and mouse anti-mast-cell tryptase monoclonal antibody (clone AA-1; Dako Japan, Kyoto, Japan). Mouse anti-basophil monoclonal antibody (clone BB-1) was generated as previously described.[17]

AKC/VKC Patient Selection and Giant Papillae Tissue Processing

Giant papillae were resected for therapeutic purposes[14] from six patients with AKC and four patients with VKC after obtaining informed consent (Table 1).AKC was defined as bilateral, chronic inflammation of the conjunctiva and lids associated with atopic dermatitis, and VKC was defined as bilateral, chronic inflammation of the conjunctiva associated with predisposition to atopy.[18] Patients who had atopic dermatitis or corneal stromal neovascularization were excluded from the VKC diagnosis. All patients with AKC or VKC were treated by topical dexamethasone eyedrops for at least 4 weeks before surgery. Some patients were also treated by an oral steroid (20 mg/day prednisolone) or by cyclosporine A eyedrops. Total serum IgE concentration and specific IgE titer against 26 common antigens (including house dust mite and Japanese cedar pollen) were measured by SRL, Inc. (Tokyo, Japan) using the fluorescence enzyme immunoassay method and the enzyme-linked immunosorbent assay (ELISA) method, respectively. Upper bulbar conjunctivae were resected from six patients with conjunctivochalasis and four patients with superior limbic keratoconjunctivitis (SLK)[19] for therapeutic purposes after informed consent was obtained (Table 2). Conjunctivochalasis was defined as a redundant conjunctiva typically located between the globe and the lower eyelid,[20] and SLK was defined according to the original clinical descriptions by Theodore.[21] Giant papillae were fixed with 4% paraformaldehyde (PFA)-phosphate buffered saline (PBS) for at least 4 hours and were then immersed in a 20% sucrose-PBS solution for 30 minutes, rapidly frozen in OCT compound (Sakura Finetek, Tokyo, Japan), and stored at −80°C. All procedures were approved by the ethics committee of Kyoto Prefectural University of Medicine, and the study was conducted in accordance with the tenets of the Declaration of Helsinki.

TABLE 2. Clinical Characteristics of Control Patients

Patient	Age (y)	Sex	Diagnosis
1	39	F	SLK
2	49	F	SLK
3	70	F	Conjunctivochalasis
4	65	M	Conjunctivochalasis
5	71	F	Conjunctivochalasis
6	74	M	Conjunctivochalasis
7	53	F	Conjunctivochalasis
8	40	M	SLK
9	75	F	Conjunctivochalasis
10	59	F	SLK

Immunohistochemical Analysis of Giant Papillae

Seven-micrometer cryostat sections were made from the specimens and air dried. Sections were then postfixed with 4% PFA-PBS. After blocking with 1% bovine serum albumin (BSA) in PBS, the slides were reacted with anti-FcεRI-β or with anti-FcεRI-γ polyclonal antibodies for 1 hour and then with Alexa 488-conjugated anti-rabbit IgG antibody for 30 minutes. For double-staining with anti-tryptase, anti-FcεRI-α, anti-basophil, or anti-CD1a monoclonal antibodies, the slides were incubated simultaneously with FcεRI-β or FcεRI-γ polyclonal antibodies and with one of the monoclonal antibodies. In the case of double immunostaining with the anti-chymase antibody, the slides were incubated with the anti-chymase antibody overnight at 4°C, and then the FcεRI-β polyclonal antibody was added and further incubated for 1 hour at room temperature. Alexa 488-conjugated anti-rabbit IgG antibody and Alexa 594 conjugated anti-mouse IgG antibody were mixed and applied simultaneously as second antibodies. For triple immunostaining using the CD1a (class, mouse IgG1), FcεRI-α (class, mouse IgG2a), and FcεRI-β antibodies, the slides were incubated with the CD1a antibody and the FcεRI-β antibody for 1 hour at room temperature. After PBS washes, Alexa 488-anti-rabbit IgG antibody, Cy5-anti-mouse IgG_1 antibody, and PE-anti-FcεRI-α (class, mouse IgG2a) were applied simultaneously for another hour. As negative controls, normal rabbit IgG (Santa Cruz Biotechnology) was used instead of the FcεRI-β polyclonal antibody at the same concentration, or the FcεRI-β IgG antibodies were preabsorbed with a fivefold excess amount of the peptide used for immunization. These slides were then visualized with a confocal laser scanning microscope (FV1000; Olympus Corp., Tokyo, Japan).

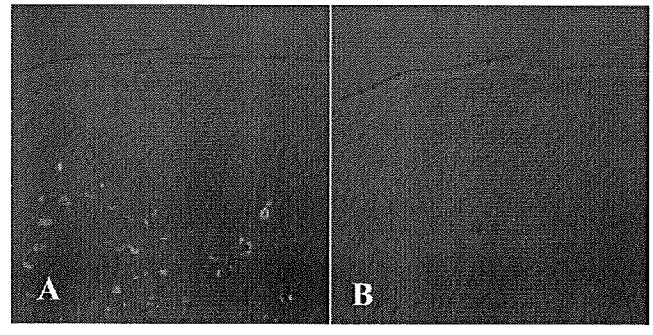

FIGURE 1. Anti-FcεRI-β immunostaining of giant papillae. Immunohistochemical staining was carried out with giant papillae specimens from patients with AKC or VKC using the anti-FcεRI-β antibody (**A**) and control rabbit IgG (**B**) at the same concentration. Original magnification, 200×. This is representative data obtained from 1 of 10 patients (patient 5 in Table 1).

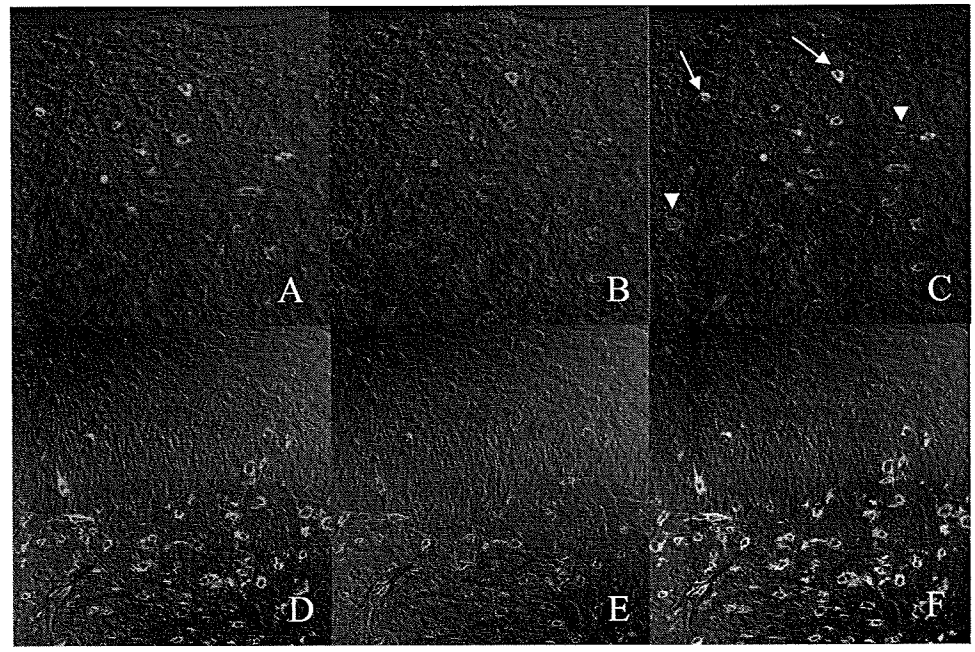

FIGURE 2. Two types of FcεRI$^+$ ($\alpha\beta\gamma_2$ and $\alpha\gamma_2$) cells in giant papillae. Immunohistochemical staining was carried out with giant papillae specimens from patients with AKC or VKC using anti-FcεRI-β (**A**, *green*) and anti-FcεRI-α (**B**, *red*) antibodies. FcεRI-β was merged with FcεRI-α (**C**). *Arrows* indicate FcεRI-α/β double-positive cells (*yellow*) and *arrowheads* indicate FcεRI-α single-positive (*red*) cells. A nearby section from the same patient was immunostained with anti-FcεRI-γ (**D**, *green*) and anti-FcεRI-α (**E**, *red*) antibodies. FcεRI-γ was merged with FcεRI-α (**F**). Original magnification, 400×. This is representative data obtained from 1 of 10 patients (patient 1 in Table 1).

Cell Counting

Numbers of FcεRI-β$^+$ and FcεRI-α$^+$ cells (membrane staining) and tryptase$^+$ cells (intracellular staining) were counted manually using 200× magnification immunostaining images. Positive cells, both in the epithelium and in the substantia propria, were counted per 1-mm unit length of the conjunctival surface as total. We counted three sections per each patient for FcεRI-β immunostaining and two sections for the remaining staining. All immunostained sections were evaluated by an observer who was blinded to the clinical data of the patients. We carried out two independent series of cell staining and counting, and we showed one representative result.

RESULTS

FcεRI-β Immunostaining of Giant Papillae and Control Conjunctivae

All the tested giant papillae samples (n = 10; Table 1) showed focal-positive immunostaining in the epithelium and in the substantia propria with anti-FcεRI-β (Fig. 1A), and the negative-control slide stained by normal rabbit IgG (Fig. 1B) and by the preabsorbed FcεRI-β antibody (data not shown) did not show any positive staining. In addition to anti-FcεRI-β staining (Fig. 2A), all the tested giant papillae showed positive staining with anti-FcεRI-α antibodies (Fig. 2B); there were FcεRI-α/FcεRI-β double-positive and FcεRI-α single-positive cells (Fig. 2C). Double-immunohistochemical staining of the nearby section shown in Figure 2A with anti-FcεRI-γ antibodies (Fig. 2D) and with anti-FcεRI-α antibodies (Fig. 2E) showed that all the FcεRI-α$^+$ cells were also FcεRI-γ$^+$ (Fig. 2F). Control upper bulbar conjunctivae from the conjunctivochalasis or SLK patients (n = 10; Table 2) showed a few FcεRI-α$^+$ cells (Figs. 3A, 3C) or a few tryptase-positive mast cells (Figs. 3B, 3D) in its substantia propria but a negligible number of FcεRI-β$^+$ cells (Fig. 3D; Table 3).

Immunolocalization and Quantification of FcεRI-β$^+$ Cells in Giant Papillae

The giant papillae were also double immunostained with anti-FcεRI-β and the antibodies to typical mast cell proteases (tryptase and chymase). FcεRI-β immunostaining was observed at the cell periphery of the tryptase$^+$ cells (Figs. 4C, 4G). Some of the tryptase$^+$ cells were FcεRI-β negative (Fig. 4C, 4G;

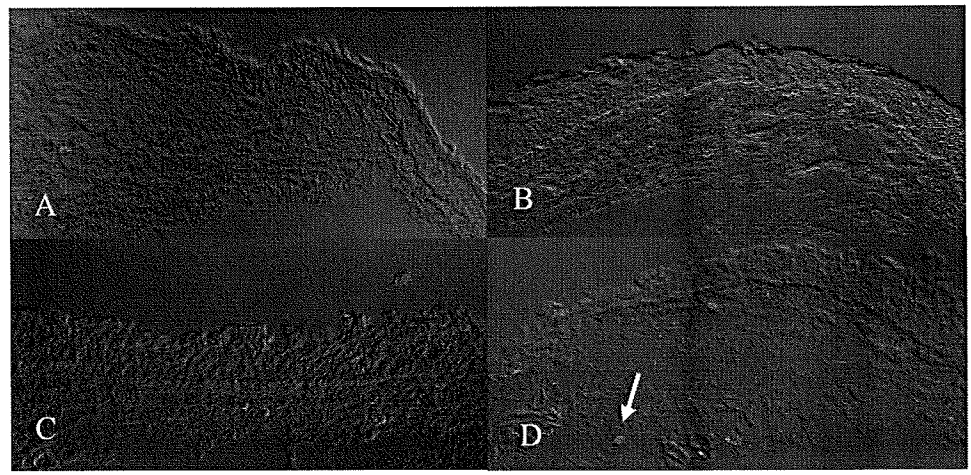

FIGURE 3. Expression of the FcεRI-β chain was almost negligible in control conjunctivae. Upper bulbar conjunctivae were obtained from conjunctivochalasis patients (**A**, **B**) and SLK patients (**C**, **D**). The conjunctivae were double immunostained with the pairs of anti-FcεRI-α (red) and anti-FcεRI-β (**A**, **C**, *green*) or anti-tryptase (*red*) and FcεRI-β (*green*) antibodies (**B**, **D**). (**D**) *Arrow* indicates FcεRI-β$^\pm$ tryptase$^+$ cells. Original magnification, 200×.

TABLE 3. Comparison of the FcεRI- and Tryptase-Positive Cells between Giant Papillae and Control Samples

	FcεRI-β^+ Cells (mean ± SD)	FcεRI-α^+ Cells (mean ± SD)	Tryptase$^+$ Cells (mean ± SD)	Ratio of FcεRI-β^+ and FcεRI-α^+ Cells (mean ± SD)	Ratio of FcεRI-β^+ and Tryptase$^+$ Cells (mean ± SD)
Giant papillae	55.9 ± 24.6*	99.0 ± 33.2†	71.1 ± 24.1‡	0.69 ± 0.08§	0.81 ± 0.13‖
Control	1.1 ± 2.3*	19.6 ± 16.9†	17.6 ± 9.8‡	0.07 ± 0.16§	0.06 ± 0.11‖

Student's *t*-test: *P = 0.0000007; †P = 0.0001; ‡P = 0.00005; §P = 0.00000007; ‖$P = 3 \times 10^{-9}$.

arrow); however, all the chymase$^+$ cells were FcεRI-β^+ (Fig. 4I, asterisks). We quantified the number of FcεRI-β^+ cells, FcεRI-α^+ cells, tryptase$^+$ cells, and FcεRI-β/tryptase double-positive cells. The numbers of FcεRI-β^+, FcεRI-α^+, and tryptase$^+$ cells were significantly higher in the giant papillae than in the control conjunctivae (Table 3). The ratio of the FcεRI-β^+ cells/FcεRI-α^+ cells in the giant papillae samples was 0.69 ± 0.08 (mean ± SD). That ratio was significantly higher than the ratio of the control samples (0.07 ± 0.16). Of tryptase$^+$ cells, 81% ± 13% expressed FcεRI-β, a rate also significantly higher than that of the control samples. Samples with hypertrophic epithelium showed FcεRI-β^+ cells predominantly at the epithelial layers (Figs. 4A, 4D, 4H). We found that intraepithelial FcεRI-β^+ cells were dominated by tryptase$^+$ and chymase$^-$ mast cells (MC_T; Figs. 4G, 4I).

We also found some FcεRI-β^+ cells within and around convoluted epithelium[22] and pseudotubules[23] (Figs. 5A, 5B; asterisks). Double immunostaining with FcεRI-β and tryptase (Figs. 5C, 5D) showed cytoplasmic tryptase staining (red) and membranous FcεRI-β staining (green). Double immunostaining with FcεRI-β and chymase (Figs. 5E, 5F) showed cytoplasmic chymase staining (red) at some of the FcεRI-β^+ cells (green). The results of the FcεRI-β^+ cell quantification are summarized in Table 3. Statistical analyses revealed that the densities of FcεRI-β^+ cells, and FcεRI-β^+-tryptase$^+$ mast cells were significantly increased in giant papillae compared with control conjunctivae. Although the average number of FcεRI-β^+ cells was higher for SLK (1.7 ± 0.7) than for conjunctivochalasis (0.7 ± 1.1) samples, the difference was not statistically significant (P = 0.38, Student's *t*-test), and the average number of FcεRI-β^+ cells in SLK samples was still significantly lower than the number of FcεRI-β^+ cells in giant papillae (P = 0.00001, Student's *t*-test).

FcεRI-β Expression in the Basophils of Giant Papillae Tissues but Not in Langerhans Cells (LCs)

During immunohistochemical analysis we found some tryptase$^-$-FcεRI-β^+ cells in the giant papillae sections, so we

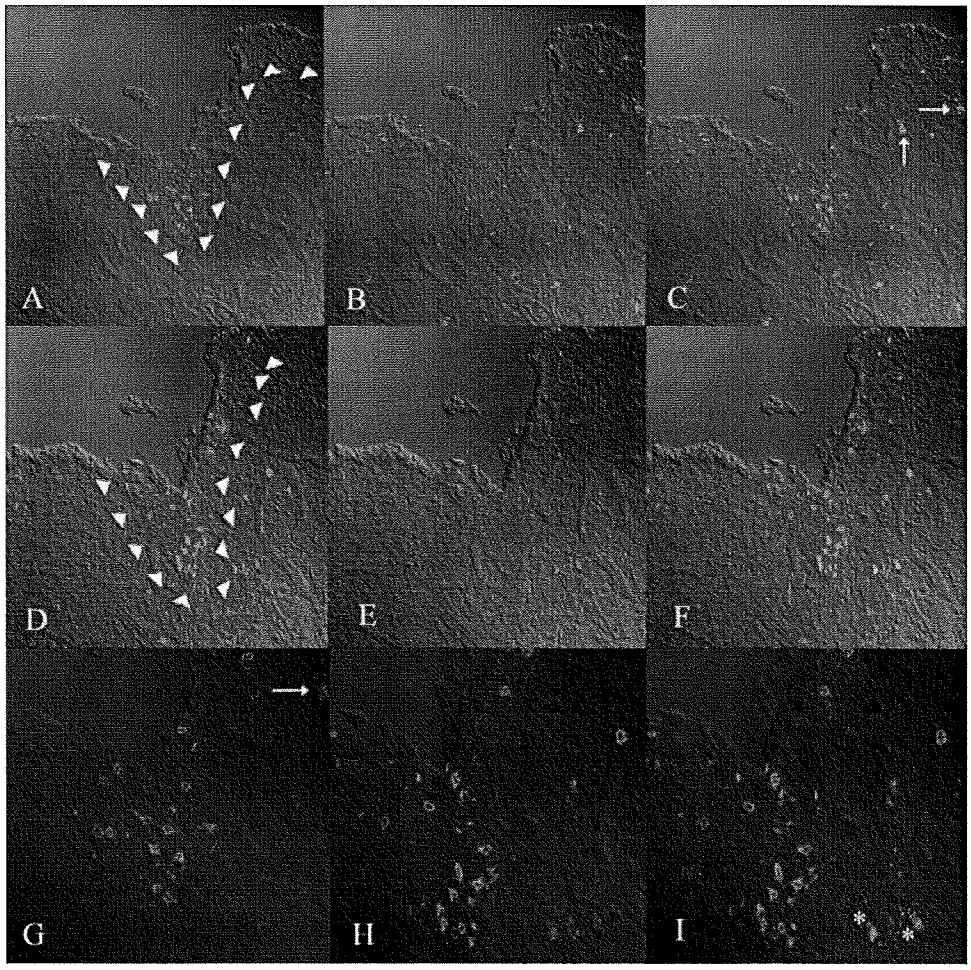

FIGURE 4. Localization of FcεRI-β^+ cells in hypertrophic epithelium of giant papillae. Giant papillae with hypertrophic epithelium were double immunostained with anti-FcεRI-β (**A**, *green*) and anti-tryptase (**B**, *red*) antibodies. FcεRI-β was merged with tryptase (**C**). Adjacent section was also double immunostained with anti-FcεRI-β (**D**, *green*) and anti-chymase (**E**, *red*) antibodies, FcεRI-β was merged with chymase (**F**). *Arrowheads* indicate the boundary line between epithelium and substantia propria. FcεRI-β immunostaining of the hypertrophic epithelial region is shown at higher magnification (**H**), and merged with tryptase (**G**) and with chymase (**I**). *Arrows* and *asterisks* indicate FcεRI-β^--tryptase$^+$ cells (**C**, **G**) and FcεRI-β^+-chymase$^+$ cells (**I**), respectively. Original magnification, 100× (**A–F**); 400× (**G–I**). This is representative data obtained from 1 of 10 patients (patient 10 in Table 1).

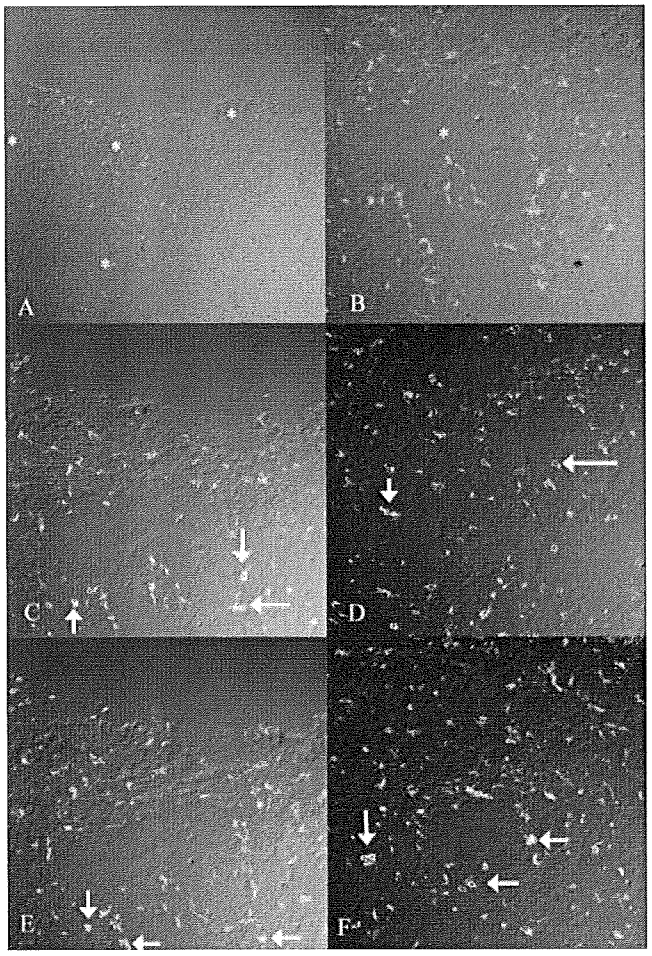

FIGURE 5. Localization of FcεRI-β^+ cells in convoluted epthelium and pseudotubules. Giant papillae with convoluted epithelium were immunostained with the anti-FcεRI-β antibody (**A**, *green*). *Asterisks* indicate convoluted epithelium and pseudotubules. The staining around convoluted epithelium (**B**, **C**, **E**) and pseudotubules (**D**, **F**) is shown at higher magnification. Some slides were double immunostained with anti-tryptase (**C**, **D**, *red*), and FcεRI-β was merged with them. *Arrows* indicate FcεRI-β^+-tryptase$^+$ cells. Adjacent sections were double immunostained with anti-chymase (**E**, **F**, *red*), and FcεRI-β was merged with them. *Arrows* indicate FcεRI-β^+-chymase$^+$ cells. Original magnifications, 100× (**A**); 200× (**B**–**F**). This is representative data obtained from 1 of 10 patients (patient 2 in Table 1).

speculated that the FcεRI-β^+ cells included basophils. Positive basophil staining was observed at the substantia propria of the giant papillae (Fig. 6A). Double immunostaining using anti-FcεRI-β and anti-basophil antibodies showed FcεRI-β immunostaining (green) at the periphery of the basophil (red) (Fig. 6C). To examine the FcεRI-receptor subtype in LCs of the giant papillae, immunostaining with CD1a and FcεRI-α/FcεRI-β antibodies was carried out. Double-staining did not reveal any CD1a$^+$/FcεRI-β^+ cells (Figs. 7A, 7C, 7E). On the other hand, two CD1a$^+$ cells were FcεRI-α^+ cells (Figs. 7B, 7C, 7D; arrows). By triple-immunohistochemical staining, we confirmed the existence of FcεRI-α^+/CD1a$^+$/FcεRI-β^- LCs (Fig. 7E, arrow) and of FcεRI-α^+/FcεRI-β^+/CD1a$^-$ mast cells (Fig. 7E, arrowhead).

Discussion

To the best of our knowledge, this study is the first to demonstrate the existence of both FcεRI-$\alpha\beta\gamma_2$and FcεRI-$\alpha\gamma_2$ receptor subtypes in the giant papillae of patients with chronic allergic conjunctivitis. FcεRI-β staining (Figs. 1, 2) showed a membranous staining pattern at the giant papillae. This staining pattern is consistent with our previous in vitro study using cultured human mast cells.[7] FcεRI-α staining of the same slide showed a broader expression at the conjunctiva than that of FcεRI-β (Fig. 2C), and all the FcεRI-α^+ cells were FcεRI-γ^+ (Fig. 2F). These findings showed the existence of FcεRI-$\alpha\beta\gamma_2$ mast cells and FcεRI-$\alpha\gamma_2$ mast cells in the giant papillae. In our previous study, we quantified FcεRI-β protein expression in human mast cells using flow cytometry.[7] We found monophasic rather than biphasic FcεRI-β expression pattern in human mast cells,[7] and Western blotting showed that the sensitivity of the FcεRI-β antibody is approximately 100 pg in the recombinant FcεRI-β protein (Matsuda A, unpublished data, 2008). These results suggested that there are various levels of FcεRI-β expression in each mast cell, and we identified an area of the mast cell population that expresses the FcεRI-β protein past the threshold as FcεRI-β-positive cells. We could not deny the possibility that FcεRI-$\alpha\beta\gamma_2$ and FcεRI-$\alpha\gamma_2$ receptor subtypes could be coexpressed in one mast cell. Nevertheless, we could conclude that there were at least two types of mast cells dominated by FcεRI-$\alpha\beta\gamma_2$ or by FcεRI-$\alpha\gamma_2$ receptors. We further examined FcεRI-β expression in the conjunctivae of two nonatopic conjunctival diseases as controls. We selected patients with conjunctivochalasis because relatively large upper bulbar conjunctivae samples could be obtained at the time of surgery. We examined patients with SLK as controls for two reasons:

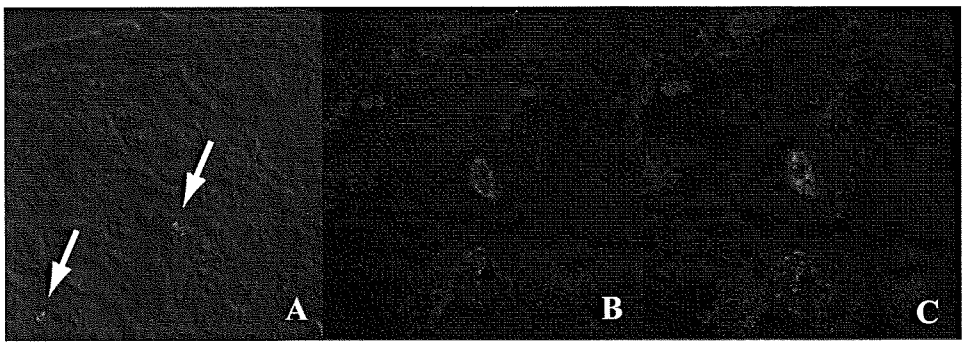

FIGURE 6. Expression of FcεRI-β in basophils of giant papillae. Giant papillae specimens from a patient with AKC (patient 6 in Table 1) were immunostained with the anti-basophil antibody (**A**; *arrows* indicate areas of positive staining). The same sections were stained with anti-FcεRI-β antibody and are shown in higher magnification (**B**). Double immunostaining using anti-FcεRI-β and anti-basophil antibodies is shown in (**C**). FcεRI-β immunostaining (*green*) was observed at the periphery of the anti-basophil-positive (*red*) cells. Original magnifications, 200× (**A**); 1000× (**B**, **C**).

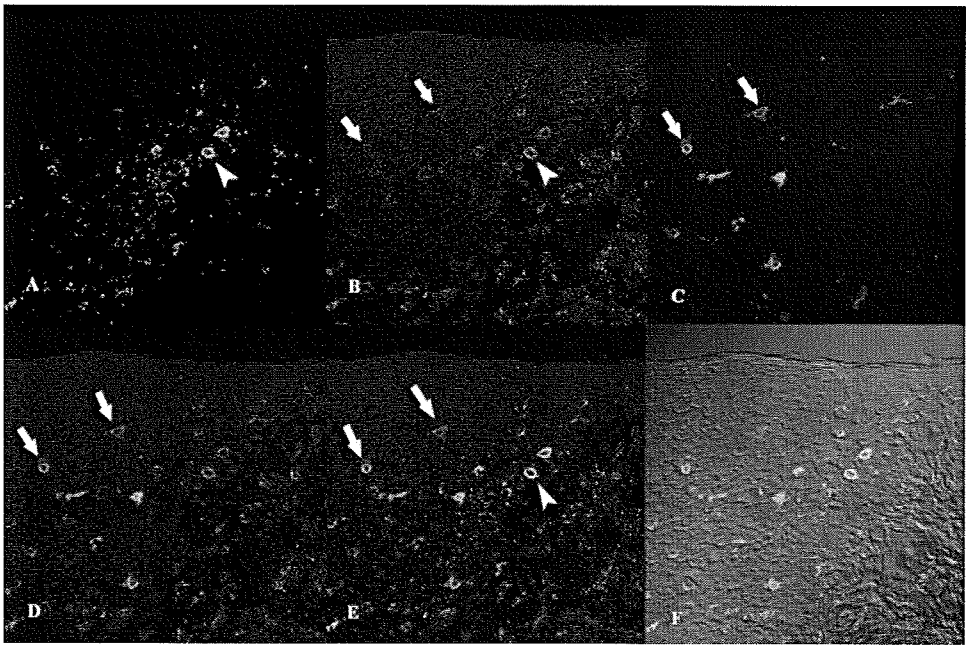

FIGURE 7. Langerhans cells in giant papillae expressing the FcεRI-$\alpha\gamma_2$ subtype. Giant papillae from a patient with AKC (patient 4 in Table 1) was stained with the anti-FcεRI-β antibody (**A**), anti-FcεRI-α antibody (**B**), and anti-CD1a antibody (**C**). Double immunostaining with the anti-FcεRI-α antibody and CD1a antibody (**D**) showed two CD1a/FcεRI-α double-positive cells (**D**; *arrows*). Triple immunostaining using CD1a (*silver*), FcεRI-α (*red*), and FcεRI-β (*green*) antibodies showed no existence of FcεRI-β/CD1a double-positive cells. $CD1a^+$/FcεRI-α^+/FcεRI-β^- LCs and FcεRI-β^+/FcεRI-α^+ mast cells (**E**, *arrows* and *arrowhead*, respectively). Merged image using a differential contrast microscope (**F**). Original magnification, 400×.

because an increased number of mast cells has been reported in the SLK conjunctivae[24] and to avoid bias from the very low number of the mast cells in the conjunctivochalasis samples. In addition, we excluded allergic conjunctivitis by careful slit-lamp examinations in these cases. The increased number of FcεRI-β^+ cells and the higher ratio of FcεRI-β^+/FcεRI-α^+ cells number in giant papillae samples suggested the preferential expression of FcεRI-β protein in chronic allergic conjunctivitis.

Double immunohistochemical staining with anti-FcεRI-β and anti-tryptase/anti- chymase antibodies showed that 81% of tryptase$^+$ cells were FcεRI-β^+, and all the chymase$^+$ cells were FcεRI-β^+ (Figs. 4, 5; Table 3). The FcεRI-β^+ rate among chymase-positive mast cells was higher than it was among among tryptase-positive mast cells; the reason for this is unknown and requires further investigation. During the analysis of double immunostaining with anti-FcεRI-β and anti-tryptase antibodies, we found the preferential localization of FcεRI-β^+ mast cells within and around hypertrophic or convoluted epithelium and epithelial pseudotubules (Figs. 4, 5). It was reported that antigen challenge in sensitized animals induced mast cell infiltration in esophageal epithelium.[25] Kitaura et al.[26] reported that a combination of antigen and IgE could stimulate mast cell migration by autocrine/paracrine secretion of chemokines. They also showed that Lyn, a signal transduction molecule associated with FcεRI-β immunoreceptor tyrosine-based activation motif,[27] plays an essential role for the antigen-IgE-induced mast cell migration. We considered the possibility that the accumulation of FcεRI-β^+ mast cells in the hypertrophic epithelium could be a reflection of increased antigen stimulation at the ocular surface of AKC/VKC eyes. Furthermore, Galli et al.[28] reported that mast cells could induce airway epithelial cell proliferation in mouse asthma models in response to antigen stimulation; hence, it is possible that the infiltrating FcεRI-β^+ mast cells themselves play some roles in epithelial hypertrophy.

This is the first study to show the existence of FcεRI-$\alpha\beta\gamma^{2+}$ basophils (Fig. 6) and FcεRI-$\alpha\gamma_2{}^+$ LC (Fig. 7) at the protein level in giant papillae. Recently, it was reported that basophils play major roles in delayed-phase allergic reaction, independently of T cells and mast cells.[29] We are now investigating the role of FcεRI-β^+ basophils in the pathophysiology of AKC/VKC. The existence of FcεRI-$\alpha\gamma_2{}^+$ LC is consistent with previous findings in mRNA levels,[30] and FcεRI-$\alpha\gamma_2{}^+$ LCs play important roles for enhanced antigen presentation in atopic disorders.

Recent studies have also indicated that the role of the FcεRI-β protein in mast cells depends on the amount of IgE-specific antigen, with the low concentration of antigen FcεRI-β chain working as an amplifier[31] but with a supraoptimal amount of antigen FcεRI-β chain acting as an inhibitory molecule for degranulation and cytokine expression.[31,32] In this study we showed preferential FcεRI-β expression in the giant papillae samples in AKC/VKC, suggesting the involvement of an FcεRI-β–mediated mechanism for amplifying reactions against chronic low concentration of antigens. Additional functional studies will be necessary for investigating the roles of the FcεRI-β chain; this antibody will be a useful tool for in situ analysis.

Acknowledgments

The authors thank Hisako Takeshita for excellent technical assistance and John Bush for reviewing the manuscript.

References

1. Kraft S, Kinet JP. New developments in FcεRI regulation, function and inhibition. *Nat Rev Immunol.* 2007;7:365–378.
2. Cookson WO, Sharp PA, Faux JA, Hopkin JM. Linkage between immunoglobulin E responses underlying asthma and rhinitis and chromosome 11q. *Lancet.* 1989;1:1292–1295.

3. Shirakawa T, Li A, Dubowitz M, et al. Association between atopy and variants of the beta subunit of the high-affinity immunoglobulin E receptor. *Nat Genet.* 1994;7:125-129.
4. Lin S, Cicala C, Scharenberg AM, Kinet JP. The Fc(εn)RIβ subunit functions as an amplifier of Fc(ε)RIγ-mediated cell activation signals. *Cell.* 1996;85:985-995.
5. Donnadieu E, Jouvin MH, Kinet JP. A second amplifier function for the allergy-associated Fc(ε)RI-β subunit. *Immunity.* 2000;12:515-523.
6. Novak N, Kraft S, Bieber T. Unraveling the mission of FcεRI on antigen-presenting cells. *J Allergy Clin Immunol.* 2003;111:38-44.
7. Matsuda A, Okayama Y, Ebihara N, et al. High-affinity IgE receptor-beta chain expression in human mast cells. *J Immunol Methods.* 2008;336:229-234.
8. Tuft SJ, Kemeny DM, Dart JK, Buckley RJ. Clinical features of atopic keratoconjunctivitis. *Ophthalmology.* 1991;98:150-158.
9. Foster CS, Calonge M. Atopic keratoconjunctivitis. *Ophthalmology.* 1990;97:992-1000.
10. Bonini S, Lambiase A, Marchi S, et al. Vernal keratoconjunctivitis revisited: a case series of 195 patients with long-term followup. *Ophthalmology.* 2000;107:1157-1163.
11. Nomura K, Takamura E. Tear IgE concentrations in allergic conjunctivitis. *Eye.* 1998;12(part 2):296-298.
12. Kocabeyoglu S, Bozkurt B, Bilen O, Irkec M, Orhan M. Serum allergen specific immunoglobulin E levels in patients with allergic conjunctivitis. *Eur J Ophthalmol.* 2008;18:675-679.
13. Abu el-Asrar AM, Van den Oord JJ, Geboes K, Missotten L, Emarah MH, Desmet V. Immunopathological study of vernal keratoconjunctivitis. *Graefes Arch Clin Exp Ophthalmol.* 1989;227:374-379.
14. Fujishima H, Fukagawa K, Satake Y, et al. Combined medical and surgical treatment of severe vernal keratoconjunctivitis. *Jpn J Ophthalmol.* 2000;44:511-515.
15. Ebihara N, Okumura K, Nakayasu K, Kanai A, Ra C. High level of Fc epsilon receptor I-bindable immunoglobulin E in the tear fluid and increased immunoglobulin E-saturated cells in the giant papillae of vernal keratoconjunctivitis patients. *Jpn J Ophthalmol.* 2002;46:357-363.
16. Donnadieu E, Jouvin MH, Rana S, et al. Competing functions encoded in the allergy-associated F(c)εRIβ gene. *Immunity.* 2003;18:665-674.
17. McEuen AR, Calafat J, Compton SJ, et al. Mass, charge, and subcellular localization of a unique secretory product identified by the basophil-specific antibody BB1. *J Allergy Clin Immunol.* 2001;107:842-848.
18. Barney N. Vernal and atopic keratoconjunctivitis In : Krachmer JH, ed. *Cornea.* 2nd ed. Philadelphia: Mosby; 2005:667-674.
19. Matsuda A, Tagawa Y, Matsuda H. Cytokeratin and proliferative cell nuclear antigen expression in superior limbic keratoconjunctivitis. *Curr Eye Res.* 1996;15:1033-1038.
20. Meller D, Tseng SC. Conjunctivochalasis: literature review and possible pathophysiology. *Surv Ophthalmol.* 1998;43:225-232.
21. Theodore FH. Superior limbic keratoconjunctivitis. *Eye Ear Nose Throat Mon.* 1963;42:25-28.
22. Morgan SJ, Williams JH, Walls AF, Holgate ST. Mast cell hyperplasia in atopic keratoconjunctivitis: an immunohistochemical study. *Eye.* 1991;5(part 6):729-735.
23. Foster CS, Rice BA, Dutt JE. Immunopathology of atopic keratoconjunctivitis. *Ophthalmology.* 1991;98:1190-1196.
24. Sun YC, Hsiao CH, Chen WL, Wang IJ, Hou YC, Hu FR. Conjunctival resection combined with Tenon layer excision and the involvement of mast cells in superior limbic keratoconjunctivitis. *Am J Ophthalmol.* 2008;145:445-452.
25. Yu S, Stahl E, Li Q, Ouyang A. Antigen inhalation induces mast cells and eosinophils infiltration in the guinea pig esophageal epithelium involving histamine-mediated pathway. *Life Sci.* 2008;82:324-330.
26. Kitaura J, Kinoshita T, Matsumoto M, et al. IgE- and IgE+Ag-mediated mast cell migration in an autocrine/paracrine fashion. *Blood.* 2005;105:3222-3229.
27. Turner H, Kinet JP. Signalling through the high-affinity IgE receptor Fc epsilonRI. *Nature.* 1999;402:B24-B30.
28. Williams CM, Galli SJ. Mast cells can amplify airway reactivity and features of chronic inflammation in an asthma model in mice. *J Exp Med.* 2000;192:455-462.
29. Mukai K, Matsuoka K, Taya C, et al. Basophils play a critical role in the development of IgE-mediated chronic allergic inflammation independently of T cells and mast cells. *Immunity.* 2005;23:191-202.
30. Bieber T, Kraft S, Jurgens M, et al. New insights in the structure and biology of the high affinity receptor for IgE (Fc epsilon RI) on human epidermal Langerhans cells. *J Dermatol Sci.* 1996;13:71-75.
31. Xiao W, Nishimoto H, Hong H, et al. Positive and negative regulation of mast cell activation by Lyn via the FcεRI. *J Immunol.* 2005;175:6885-6892.
32. Gimborn K, Lessmann E, Kuppig S, Krystal G, Huber M. SHIP down-regulates FcεR1-induced degranulation at supraoptimal IgE or antigen levels. *J Immunol.* 2005;174:507-516.

眼科手術 22：349-351，2009

森式直立型手術用ゴニオレンズ（森ゴニオレンズ）

森　和彦*

森式直立型手術用ゴニオレンズ（森ゴニオレンズ；Mori Upright Surgical Goniolens）は内蔵するダブルミラーと中央部視野により，眼球や頭部を傾斜させることなく視軸方向から全周の隅角を確認・操作できる手術用隅角鏡である．

はじめに

従来の手術用隅角鏡は視軸方向から隅角を観察できないため，隅角手術時に全周の隅角を操作するには，その都度，顕微鏡，眼球もしくは頭部を目的とする方向へ傾斜もしくは回旋させねばならず，手間と時間がかかるとともに結果として無駄な操作も多くならざるをえなかった．今回，筆者らが考案した森式直立型手術用ゴニオレンズ（森ゴニオレンズ）(Mori Upright Surgical Goniolens，オキュラー社；**図1**）は，内蔵するダブルミラーと中央部視野により視軸方向から全周の隅角を確認・操作できるものである．

I　原理と特徴

森式直立型手術用ゴニオレンズ（森ゴニオレンズ）には以下の2つの特徴がある．第1は岩崎ら[1]のコンセプトをもとに内蔵した2枚のミラーにより眼球を傾斜させることなく視軸方向から隅角を観察・操作可能である点，第2は隅角鏡を回転しても手術器具の位置が確実に把握できるように中央部視野を確保した点である．ダブルミラーを介した光路と中央部の光路の2つの光路が存在する（**図2**）ため，隅角を明るく照明できるのみならず器具の陰影も形成されなくなり，より視認性に優れた隅角像を得ることができる．さらに隅角鏡の角膜接地面に切り込みが入れてある（**図2**青矢印）ために，隅角切開刀や隅角癒着解離針などの器具を挿入しても隅角鏡が安定して角膜面に接している．唯一の欠点としては直接型隅角鏡（Swan-Jacob Gonioprism）と比較して（**表1**）拡大率においてやや劣るために手術用顕微鏡の倍率を最大倍率まで拡大する必要があり，全周を確認するためには輪部に沿って顕微鏡を大きく移動させていかなくては

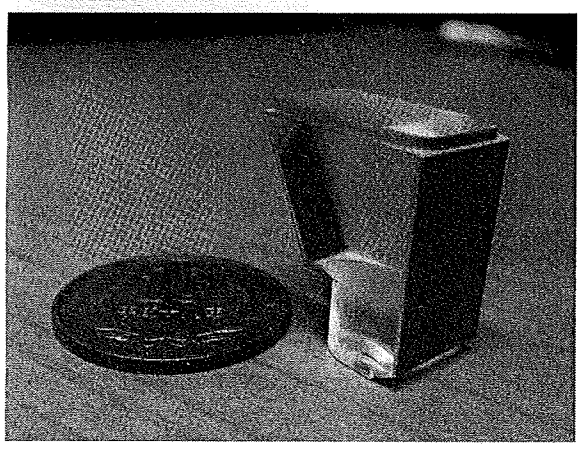

図1　森ゴニオレンズ

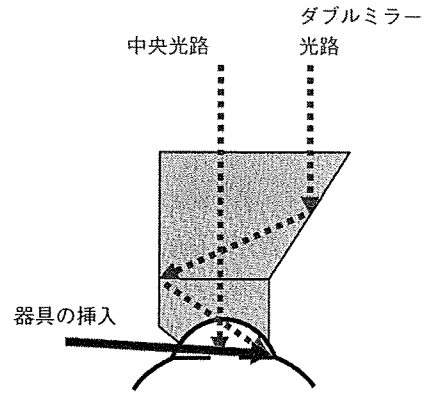

図2　森ゴニオレンズの光路図

* Kazuhiko Mori：京都府立医科大学大学院医学研究科視覚機能再生外科学（眼科学教室）
〔別刷請求先〕森　和彦：〒602-0841 京都市上京区河原町通広小路上ル梶井町465　京都府立医科大学大学院医学研究科視覚機能再生外科学（眼科学教室）　e-mail：kmori@koto.kpu-m.ac.jp

0914-6806/09/ ¥100/ 頁 /JCOPY

表1　手術用隅角鏡比較のまとめ

	Swan-Jacob Gonioprism	Mori Upright Surgical Goniolens
特徴	直像型	ダブルミラー型
観察方向	視軸に対し約45～60°	視軸方向
眼球および頭位	傾斜	垂直
全周隅角操作	上下は困難	容易
滅菌	オートクレーブ	EOGガス滅菌，グルタルアルデヒド

ならない点がある（図3）．

II　手術用隅角鏡を利用する術式と利用法

次に実際に森ゴニオレンズを利用する術式とその利用法について述べる．一般的に緑内障手術において最も森ゴニオレンズを利用する可能性の高い術式としては，隅角切開術と隅角癒着解離術が挙げられるが，それ以外にも線維柱帯切開術時のプローブの確認目的やtrabecutomeなどの新しい手術においても使用することが可能である．通常，隅角手術時には森ゴニオレンズを角膜上に載せ，片手で把持しつつ他方で器具を操作して行う（図4）．

1．隅角切開術（goniotomy）と隅角癒着解離術（goniosynechialysis）（図5）

いずれも全周にわたって隅角を確認しながら隅角切開もしくは癒着解離を施行する必要がある．従来の直接型隅角鏡では眼球と頭部，顕微鏡を大きく傾斜させ眼球を回旋させながら1象限ずつ行う必要があったが，森ゴニオレンズではこれらを傾斜もしくは回旋させる必要がなく，単なる隅角鏡の回転のみ（図3）で全周の隅角の確認・操作が可能である．通常はゴニオレンズを角膜上に載せる前に輪部に3カ所のサイドポートを作製し，サイドポートから器具を挿入した後にゴニオレンズを載せ，約120°の範囲にわたる隅角の操作を行う．

これらの手術における最大のポイントは視認性の確保であり，隅角の微細構造がしっかりと見えている状態で操作を行うことで，隅角後退や前房出血の頻度を低下させうるのみならず，器具の接触による角膜内皮障害も防ぐことができる．角膜と隅角鏡の間隙に血液が迷入するだけでも視認性が著しく損なわれるため，麻酔の際にも可能な限り出血させない心がけを行うのみならず，角膜上に粘弾性物質を置いたり，常に水を流し続けたりするなど，接触面に血液が迷入しない方策が必要である．また白内障との同時手術の際には，可能な限り先に隅角の操作を行ったほうが，良好な角膜の状態であるためにより視認性に優れている．

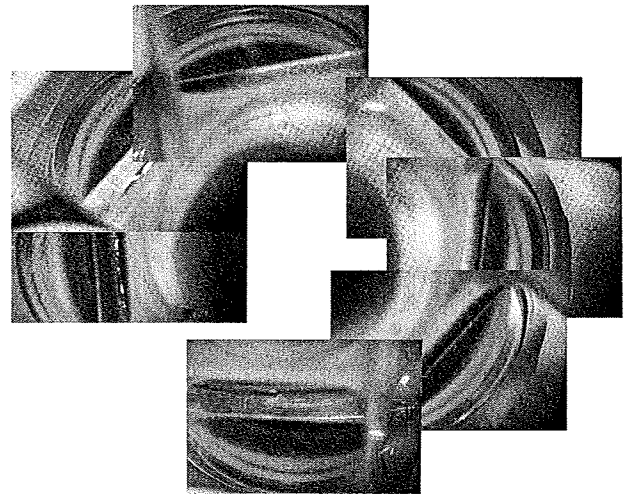

図3　隅角鏡の回転による全周隅角の確認

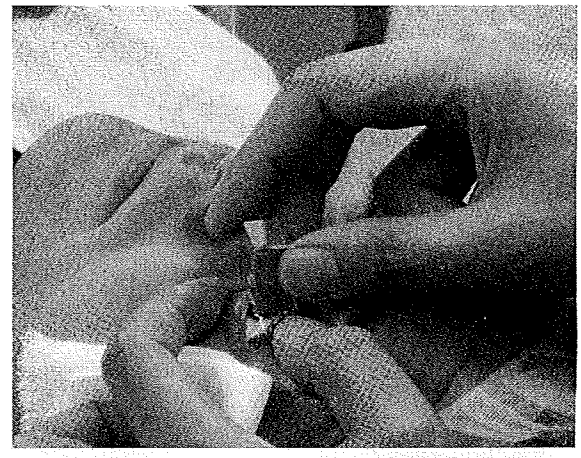

図4　ゴニオレンズの把持

第2のポイントは前房の保持である．前房という限られた空間で器具を操作する必要があるため，粘弾性物質のなかでもできれば分子量の大きいものを用い，前房深度を十分に確保することが必須である．また隅角操作中